ADDIS ABABA UNIVERSITY

SCHOOL OF EARTH SCIENCES

TITLE: PETROGENESIS AND SOURCE ROCK CHARACTERIZATION OF VOLCANIC ROCKS FROM THE GIDOLE HORST IN THE SOUTHERN ETHIOPIAN RIFT

By Asmamaw Hangibayna

A thesis submission to school of Earth sciences Addis Ababa University in partial fulfillment of the requirements for a masters degree in Geochemistry

Advisor: Prof. Dereje Ayalew

Co-advisor: Prof. Asfawossen Asrat

Addis Ababa University, Ethiopia

September, 2021

ADDIS ABEBA UNIVERSITY

SCHOOL OF GRADUATE STUDIES

SCHOOL OF EARTH SCIENCES

Petrogenesis and source rock characterization of volcanic rocks from the Gidole horst in the southern Ethiopian rift

BY Asmamaw Hangibayna

Professor Dereje Ayalew		11/10/2021
Advisor	Signature	Date
Dr. Balemwal Atnafu	_____	___/___/____
Chairman School of Earth Science	Signature	Date
Professor Gezahegn Yirgu		11/10/2021
Examiner	Signature	Date
Professor Bekele Abebe		11/10/2021
Examiner	Signature	Date

Addis Ababa, Ethiopia

September 2021

Declaration for Originality

I hereby declare that the thesis entitled “Petrogenesis and source rock characterization of volcanic rocks from the Gidole horst in the southern Ethiopian rift” is my original work prepared for the partial fulfillment of Master Degree of Geological Science in Geochemistry, School of Earth Sciences, Addis Ababa University during the year of 2021 under the supervision of Professor Dereje Ayalew. I declare that this work is not presented and published anywhere else, and all sources of material used for this thesis work have been duly acknowledged.

Asmamaw Hangibayna Kussita  11/10/2021

MSc candidate Signature Date

This is to certify that the above declaration made by the candidate is correct to the best of my knowledge.

Prof. Dereje Ayalew 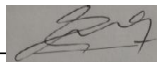 11/10/2021

Advisor Signature Date

Abstract

The eastern branch of East African rift system consists of Ethiopian and Kenyan rift systems. Ethiopian rift system start from the afar triple junction to the broaden zones of the over lapping rift systems segmented into three parts the northern, the southern and the central rift system. Gidole horst lies in the complex zone of the overlapping Ethiopian and Kenyan rift in the southern part of Ethiopia. It is bounded between Chamo basin to the East and Woyto basin to the west nearly orient in southeast-northwest direction. It has step up normal faults rise to an elevation 2540m above mean sea level.

To constrain the petrogenetic evolution and source rock characterization of the Gidole horst volcanic rocks; integrated field, petrographic analysis and major and trace element geochemistry has been conducted. Thus, the study constrained petrogenesis of volcanic rocks and their association through petrographic, major and trace element data, and the source rocks of the basalts and the rhyolites through trace element models. The possible contamination of the basalts and the rhyolites were also addressed.

The stratigraphic studies in the Gidole horst allowed the recognition of several phase of volcanic activity. The lowest exposed unit is the lower basalt equivalent to the Amaro horst lying over the metamorphic basement exposed around Gato. This unit has several phases of eruption and is overlain by felsic tuff. Felsic tuff consists of the lower ignimbrite and the upper unwelded tuff. It is sandwiched between the lower basalt and the middle basalts, where the middle basalts are characterized by columnar joints. A thin trachytic flow over lays the middle basalts around Gebele-Beno, specifically in Himbro expected to be the volcanic vent. The existence of mud stone overlaying these units indicates the presence of hiatus between the trachytic flow and the upper basalts. The upper basalts cover a large volume and the upper flows fall in the sub-tropical climate condition that are highly altered.

Petrographically the rocks are classified as olivine-plagioclase phyric, aphyric, trachytic and felsic tuff. The very early flows of lower basalts show olivine-plagioclase phenocrysts with microphenocrysts of olivine, plagioclase and pyroxene. The groundmass of it consists of opaque’s in addition to the above minerals. Whereas, the upper flows of the lower basalt, the middle basalts are aphyric consists olivine, plagioclase, pyroxene and opaque minerals with less

amphibole observed in the upper basalts. The trachyte show trachytic texture with plagioclase and plagioclase is absent in felsic tuff, instead large crystals of sanidine are observed.

Major and trace element variation of Gidole horst volcanic rocks show strong association of the rocks and support the origin of the evolved rocks by crystal fractionation starting from the lower basalt to the more evolved products. The separation of olivine, plagioclase, pyroxene and opaque occurred in the basaltic rocks and addition of sodic plagioclase in the intermediate trachyte. Furthermore, the evolution generated strong enrichment of incompatible elements and depletion in compatible elements during the course of the fractionation. As a result the more evolved rhyolite have higher concentration of incompatible elements (e.g. Zr, Rb, Th, Ta and REE) and lower concentrations of compatible elements (Ni, Cr, Sr and Ba). As Ba and Sr substitute Ca in plagioclase, they are readily compatible to the early formed mineral, which is plagioclase. Consequently, Ba and Sr formed peak in the mantle normalized diagrams specifically in the lower basalts. Whereas the evolved produces, produce a trough for those elements. In addition to this, the rhyolites have a trough for P and Ti indicating the fractionation of apatite and Fe-Ti oxide.

The strong correlation between the volcanic rocks shown on the petrographic analysis, major and trace element variation diagrams, the volcanic rocks of Gidole horst have shared comment source rather than displaying different sources. Thus, the lower basalt is the oldest and primitive basalt from which the other basalts and felsic rocks are evolved. Based on the strong fractionation of REE the model was introduced to determine the source of the rock and indicates they were derived by relatively small degrees of partial melting of a source in which, garnet remains as a residual. Even though they share common source there are some differences observed among the rocks. This is due to the contamination with rocks occurred during the rout to the surface below the upper crust.

Acknowledgment

We would like to thank God that helped me in everything to complete the work effectively.

Ii is my pleasure to express a great gratitude to prof. Dereje Ayalew my advisor for his helpful advice, indispensable suggestion and above all correcting and reviewing this paper, and to prof. Asfawossen Asrat for his willingness to advice, constructive comments during report writing and assistance to select the samples for thin section and geochemical study. I would also thank DejeneTeka for his finical support during sample analysis, and Tarku Jaleta for his support in Geological survey. It is also my pleasure to express my gratitude for my classmate friends, especially Getie Berlie, Nazeridin Kenzu, Natinael Kasa and Faysal Seifu for their technical supports.

Especial thanks for Addis Ababa University partly funding this thesis and thanks to Arba Mich University, College of Natural Sciences, and Department of Geology for access of materials, like Camera, GPS and Brunton compass, and petrographic studies. I also like to thank department head Mr. Abel Abebe for his willingness to prove those materials.

Finally, I would like to thank, provide dignity to Derashe society for their love-interaction and permit to use different access in their premises.

Table of Contents

List of Figure

List of table

Acronyms

MORB = Mid Oceanic Ridge Basalts

OIT = Ocean Island Tholeiites

OIB = Ocean Island Basalts

LILE = Large Ion Lithophile Elements

HFSE = High Field Strength Elements

REE = Rare Earth Elements

E-MORB = Mid Oceanic Ridge Basalts

E-W = East-West

N-W = North-West

LT = Low Titanium

HT = High Titanium

ICP-AES = inductively coupled plasma atomic emission spectrometry

ICP-MS = inductively coupled plasma mass spectrometry

HCL = hydrochloric acid

LOI = Loss on Ignition

Chapter one

1. Introduction

1.1 Background and justification

The main Ethiopian rift is one of the active rifts in Africa extending from the Afar Depression southwards to a broad zone of basins and ranges near the Ethiopian border with Kenya (Davidson, 1983; Ebinger et al, 1993,). It has three segments: northern, central and southern segments where the segments are separated by roughly E-W trending transverse structures (Philippon et al., 2014). The southern rift start from the Goba-Bonga lineament [Abbate and Sagri, 1980]and began to broaden south of Lake Abaya (Ganjule basin) (Ebinger et al, 1993). It has an overlap of the northward propagating Kenyan rift and southward propagating Ethiopian rift between Lake Turkana and Lake Chamo (Giday WoldeGabriel and Aronson, 1987; Rooney 2010) the overlap region is called 'broadly rifted zone' with numerous horsts and grabens over the 300 km rift width (Davidson,1983; Giday Woldegabriel and Aronson, 1987).One of the horst among those horsts is Gamo-Gidole horst (Ebinger et al., 1993) bounded within Chamo basin and Woyto basin that has a series of step up faults rises to an elevation of 3000m.

In Southern Main Ethiopian rift before the start of rifting (extension) at about 15-20Ma (Pik et al., 2008) there is an extrusion of transitional tholeiitic flood basalts between 45 and 35 Ma and felsic eruption(s) at about 37Ma that blanketed much of the southern Ethiopian plateau region with a felsic tuff unit(Ebinger, et al., 1993). These eruptions predate the Ethiopian traps by ~15Ma and have been divided in to two magma groups: the older Amaro basalts being overlain by the Gamo basalts (Rogers, 2006). A second phase of flood basalt occurred between 18 and 11Ma (Ebinger et al., 1993), is related to the rifting, basin subsidence, and rift flank uplift. These two phases of flood basalt are distinct in both trace element &isotope ratios. The distinctive chemistries of the two eruptive phases record the tapping of two distinct source regions: a mantle plume source for the Amaro/Gamo phase and an enriched continental mantle lithosphere source for the Getra-Kele Phase (George and Rogers,2002)

Most works focus on the Amaro horst and Gamo Mountains (Levitte et al., 1974; Ebinger, et al., 1993; George and Rogers, 2002). Gidole horst has step up normal faults and sequences of volcanic rocks on the border faults. It has N-W trending alignment where Gamo highlands have N-E alignment similar with Amaro horst. Therefore, it is very interesting to carry a research on

Gidole horst and correlate with Amaro basalts that were well studied before by those authors (Levitte et al, 1974, Ebinger et al, 1993, George and Rogers 2002, Rooney 2010).

1.2 Description of the study area

1.2.1 Location

The Gidole horst is located in Southern Ethiopia, specifically in the South Nation Nationalities and Peoples Regional State, in DerasheWoreda~500kms from Addis Ababa capital city of Ehiopia. Geographically the study area is bounded between two basins: Chamo basin to the east and Woyto basin to the west (Fig 2.1).It covers an area of approximately 270km^2 and connected to the Gamo mountains to the north.

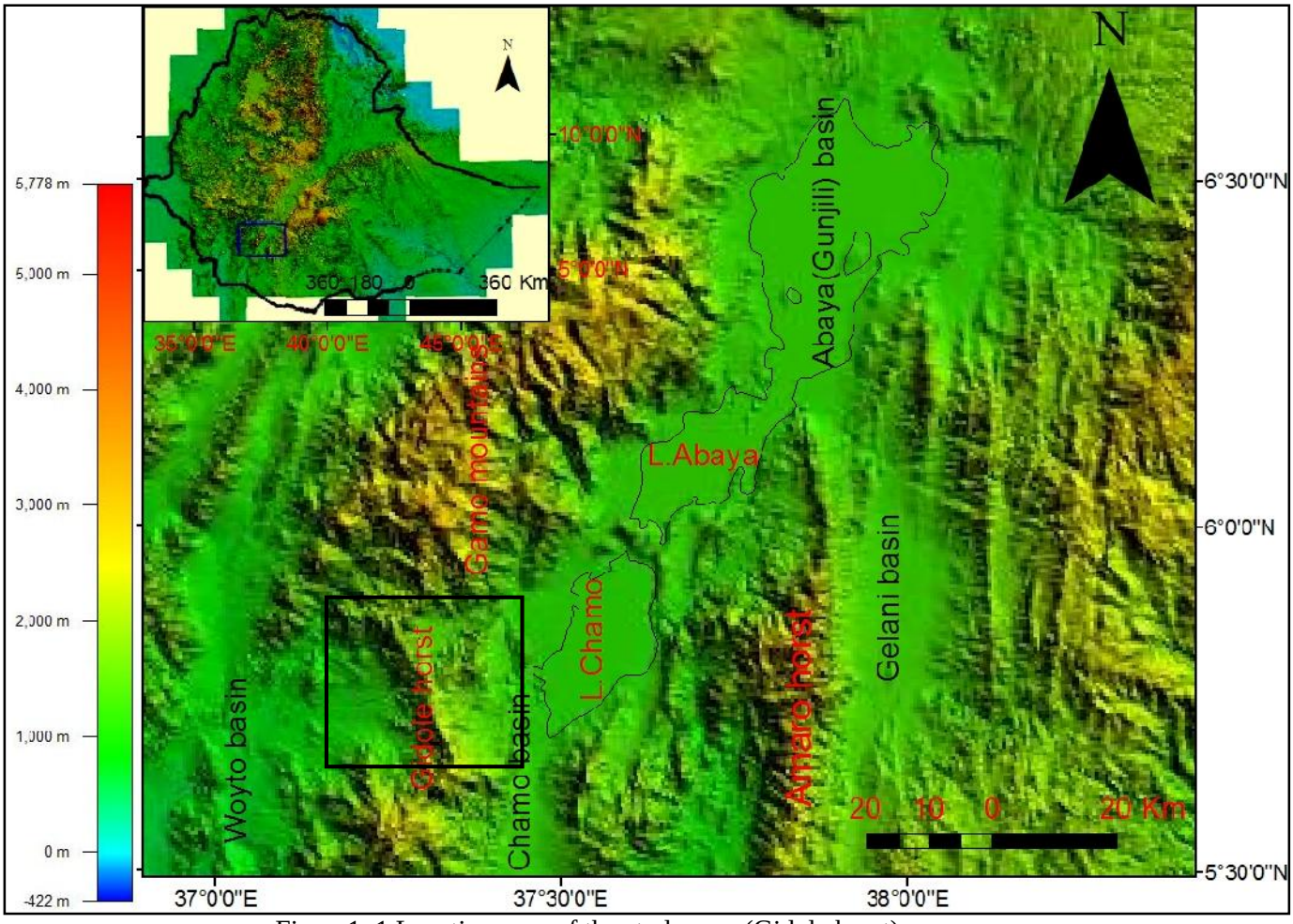

Figure1. 1 Location map of the study area (Gidole horst)

1.2.2 Accessibility

The study area has accessed from Arba Minch through the Arba Minch –Konso main road that passes on the Chamo basin and Arba Minch – Gidole and then to Gato asphalts roads. Moreover, many gravel roads and foot trails give an access to the area for the individual traverses (Fig 1.2).

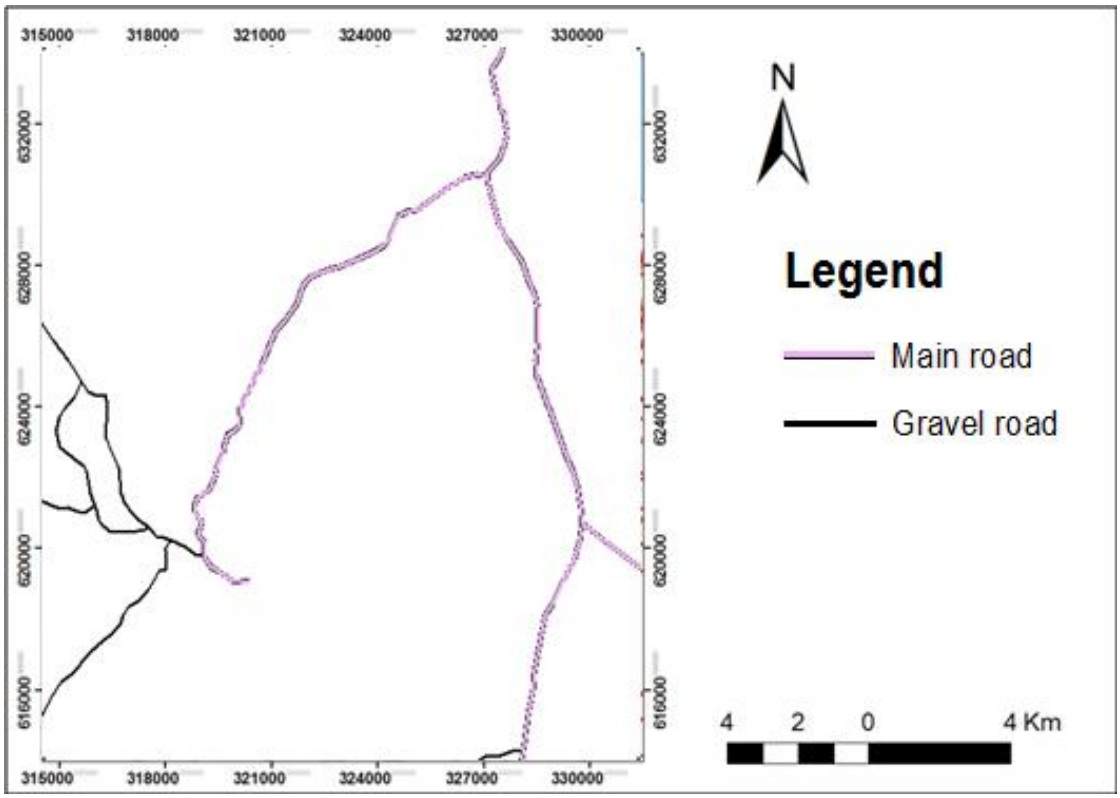

Figure1. 2 Accessibility map of the study area

1.2.3 Physiography and Relief

The Gidole horst has a series of ridges that start with the heist elevation near the Gardula summit with nearly N-E direction and, bend to the N-E direction with decreasing elevation to the North until it connected with N-E trending Gamo highlands. The Eastern side of Gidole horst has step up series of normal faults start from Chamo basin to the Gardula summit. However, the western side has steeper escarpments and has less normal faults compared to the Eastern side.

Compare to the Gamo-Mountains and Amaro horst the Gidole horst has low relief with highest elevation at the Gardula summit and lowest elevation in the Chamo and Woyto basins. The

overall relief of the study area is about 1440m (i.e. highest elevation of 2540m in the Gardula summit and the lowest elevation of 1100m in the Chamo Lake)

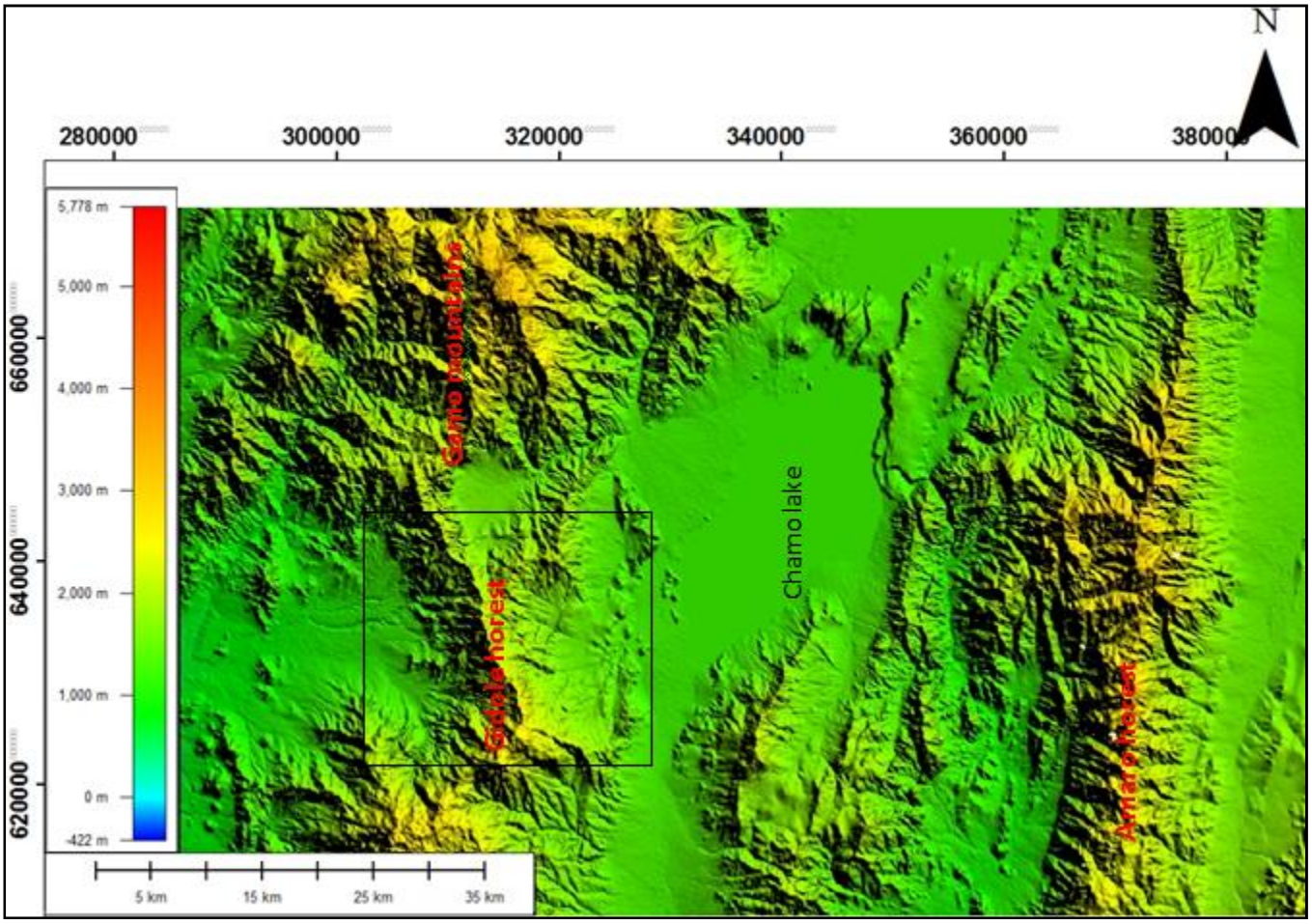

Figure1. 3 Physiographic map of the study area

1.2.4. Climate and Drainage system

The study area is has two climatic condition as the climatic condition varies with altitude. At the lowest elevation on the Chamo and Woyto basins at about 1100m it has tropical, which is called "kola"(in Amharic) climatic condition and, at highest elevation around Gidole town has subtropical or "winadega" climatic condition.

The major rivers in the study area are Kitawe and Wezeka, which flows throughout the year and feed by many small tributaries flowing from all directions. The drainage pattern of the study area is generally dendritic (Fig 1.4).

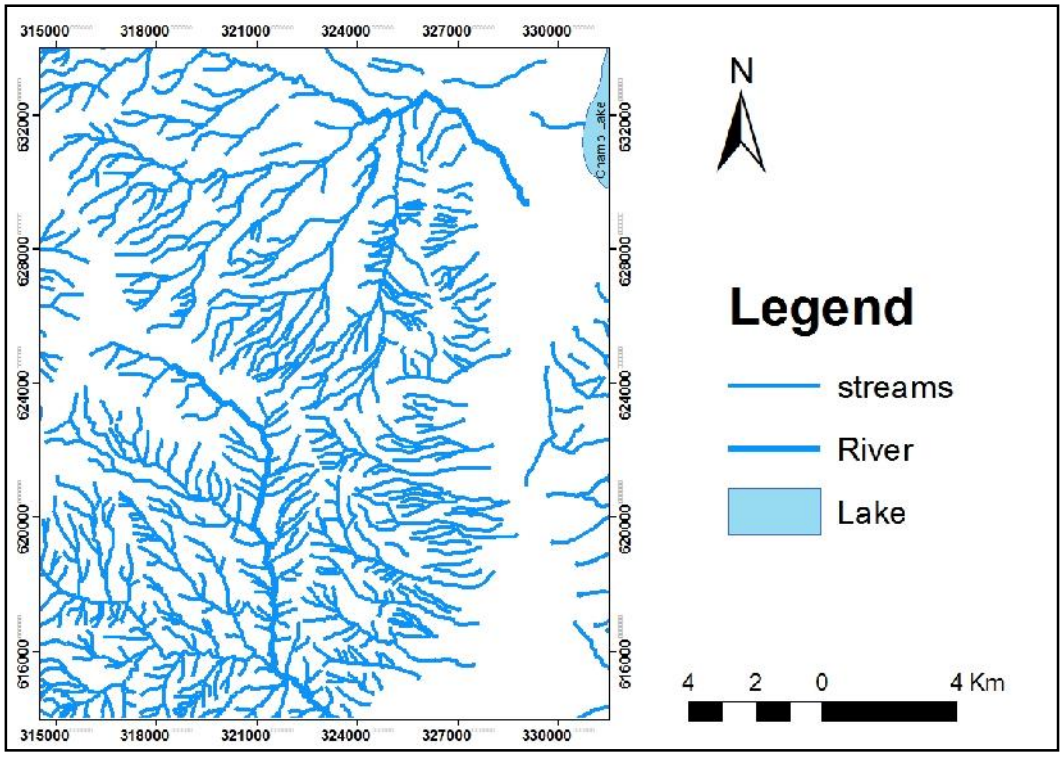

Figure1. 4 Drainage pattern map of the study area

1.3. Significance

Regionally all areas are accessed through different projects in our country (Davidson A, 1983; Ebinger et al., 1993; 2001, Rooney 2010). As those projects are regional (Davidson A, 1983) and some give their emphasis on Amaro horst (Ebinger et al., 1993; 2001) that bifurcate the main southern rift into to basins and therefore, literatures about the study area are not extensive. Even if those studies try to touch about the area, they have not given an emphasis on the petrogenesis and source rock characterization. Therefore, in this research petrogenesis and source rock characterization will be studied well at small scale to contribute for the scientific community.

As an academician, the research will help our institution Arba Minch University for igneous terrain mapping, which is previously carried at every year around Adama. After the investigation of this area, it will be one of the igneous terrain mapping where it minimize the distance and transportation cost. This research also benefits me through enhancing my experience and capacity to carry other projects.

Since the work is systematic and detail, it will benefit the community and society through inspiring others to carry their research and will be data source for academicians and other investigators.

1.4. Objectives

1.4.1 General objective

- The major objective of this study is constraining the petrogenetic evolution and source rock characterization of the Gidole horst volcanic rocks using geochemical and petrological methods.

1.4.2 Specific objectives

- Constructing and characterizing stratigraphic logs on either side of the horst
- Conducting detailed petrographic study
- Constraining the petrogenesis of the rocks using major and trace element geochemistry and petrographic studies
- Characterizing source of the volcanic rocks

Chapter two

2. Literature review

2.1. General

Ethiopian rift system cuts the uplifted Ethio-Somali plateau connected to Red sea-Gulf of Aden constructive plate boundary via Afar triple junction. There rift system start from the Afar triple junction runs through the Ethiopian floor in the south-southwest direction connected to the Kenyan rift in the southern Ethiopian rift forming a complex zone.

The main Ethiopian rifting compared to Kenyan rift, has intermediate degree of extension where both lithospheric and sub-lithospheric contributions were observed, & crustal assimilation occurs in some cases (Furman, 2007). The main Ethiopian basalts are dominantly transitional-tholeiitic falling close to the boundary between alkali basalts and olivine tholeiites (e.g. George & Rogers, 2002; Rogers, 2006), where the evolved products encompassing primarily rhyolites and trachytes. According to Arndt et al., (1998) tholeiitic magma was more susceptible to crustal contamination than alkali magmas due to volatile content difference in comparison.

The earliest most volcanic activity occurs in Southern Ethiopian between 35 and 45Ma followed by the eruption of Ethiopian flood basalts or traps erupted between 31 and 29 Ma (Rogers, 2006) that cover a large area. In the case of Rooney (2019), both flood basalts grouped u6t7nder the incompatible trace element depleted family of magmas (Type I) specifically, the Eocene Amaro basalt and the low titanium (LT) Oligocene flood basalt from NW Ethiopian plateau. He conclude that Type I lavas are not observed in the EARS post Oligocene and its origin is associated with a mantle plume. The Ethiopian flood basalt or traps compositionally has both tholeiitic (e.g., LT) and alkaline (eg.HT1 and HT2) nature (Kieffer et al., 2004) overlain by shield volcano between 10 and 23Ma. According to Furman (2007), the southwest Ethiopian magmatic province is characterized by episodic volcanism that becomes increasingly silica-under saturated through time. Rooney (2019) associate this shift in magma compositions from more silica-saturated to silica-under saturated with a decrease in the degree of extension. However, he argued that the initial melts in the rift exhibit silica-under saturation reflecting the initial destabilization and thinning of the lithospheric mantle while subsequent eruption after

lithospheric thinning, the trend towards silica-saturated compositions reflects melting of the sub-lithospheric (i.e. convicting) mantle.

The southern Ethiopian flood basalt occur in two eruption episodes: the pre-rift Amaro & Gamo transitional tholeiite (45-35Ma) and syn–extensional Getra-Kele alkali basalts between 11 and 19Ma (Ebinger et al., 1993; George and Rogers,2002).These volcanic episodes shows a distinct feature based on the interpretation of trace element & isotope ratios by George and Rogers, (2002) and conclude that the distinctive chemistries of the two eruptive phases record the tapping of two distinct source regions: a mantle plume source for the Amaro/Gamo phase and an enriched continental mantle lithosphere source for the Getra-Kele Phase. In contrast to the above, Kieffer et al. (2004) argue that the alkali basalt from Northern Ethiopia does not come from the lithospheric melt rather it come from sub-lithospheric source that was heterogeneous in terms of temperature, or composition, or both. Therefore, Kieffer et al. (2004) suggested the contamination –corrected tholeiites and HT2 alkaline lavas to have similar sources since they show similarity in isotopic composition.

The east African rift system has two plume sources: the East African and Afar plume (George and Rogers, 2002). The Afar plume is thought to be a source for volcanic rocks of the main Ethiopian rift except the Amaro and Gamo basalt in Southern Ethiopia where they are the first manifestation of magmatism from East African plume (Roger, 2006). These flood basalt is synchronous with NE-SE striking Kalisut-Lokichar rift system of northwestern Kenya to the south-west of southern Ethiopia during Eocene age. After a large hiatus, the second flood basalt (Getra- Kele basalt) in southern Ethiopia has occurred between 18 and 11Ma near to the main Ethiopian basalts and was suggested to be the afar plume (e.g. George and Rogers, 2002)

2.2. Volcanism and Stratigraphy in southern Ethiopia

Volcanism in Ethiopia started in southern Ethiopia at Eocene age before rifting has been occurred. The eruption of first flood basalt in southern Ethiopia occurred between 45 and 35Ma with an extrusion of ~500m thick sequence of volcanic rocks around Amaro horst and become thicker towards the Omo region the south west of Ethiopia (Davidson, 1983). These thickenings to the south west of southern Ethiopia indicate that the rift system could have been the main locus of magmatism and extension during Eocene (Bosworth & Morley, 1994; George and

Rogers 2002). Southern Ethiopian basalts have been divided into two magma groups: the Amaro basalts and Gamo basalts (Ebinger et al., 1993; George and Rogers, 2002). After first flood basalt there is felsic eruption(s) at 37Ma blanketed much of the southern Ethiopian plateau region with a felsic tuff unit (Ebinger et al., 1993). These felsic eruptions are evolved products and they terminated the first period of volcanism.

The second magmatism associated with extension across the Main Ethiopian Rift (MER) begins at 19 Ma, continuing to 11 Ma (Ebinger et al., 1993) after the Amaro and Gamo basalts. These alkaline basalt and trachyte volcanism is evident as flows over paleosoils and volcanoclastic sediments of the preceding magmatic cycle and, appears to be volumetrically less significant in comparison to the previous eruption (Rooney, 2017a) in that it occurred as shield volcanoes or isolated flows rather than building a thick basaltic piles . The characteristics of Quaternary volcanism in the Arba Minch region highlight that the lithospheric magmatic pathways and the mantle melting columns from which the rift basalts are derived, are strongly influenced by progressive rifting and lithospheric thinning (Rooney, 2010).

According to Levitte et al.,(1974) in the stratigraphy of Amaro horst Precambrian rocks of metamorphic basement are exposed along a narrow up faulted crustal silver forming the summit ridge of the northern part of the Amaro horst, and across the width of the horst in Central and Southern parts. Well-indurated, iron-stained conglomeratic sandstones, lacking volcanic clasts, unconformably overlie metamorphic basement along the length of the Amaro horst(Ebinger et al, 1993). This sand stone thought to be erosional product of basement rocks deposited in Tertiary time (e.g. Davidson, 1983; Ebinger et al., 1993).Thus, Ebinger et al. (1993) put the stratigraphy volcanic rocks on the conglomeratic sandstones as three phases based on their age.

(1) Eocene-Oligocene volcanic rocks where Amaro basalt that overlie red sandstone is unconformably overlain by Arba Minch felsic tuff exposed along the western Chamo border fault. The Arba Minch tuff, where seen is overlain by the Gamo porphyritic olivine basalts. The widespread Amaro tuff unit is composed of welded rhyolitic ignimbrites commonly overlain by, or interbedded with, ash-fall tephra, pyroclastic breccias, and lapilli-fall deposits (Yemane&Yohunie1987).

(2) Neogene volcanic rock starts from Getra-Kele unit, which is separated from the Amaro tuff by an angular unconformity. Getra-Kele basalts are interbedded with fluvio-lacustrine strata containing pumice clasts along the Gamo-Gidole horst. Trachytic-syenitic volcanic plugs intrude basement and overlying Palaeogene basalts, and lie along border fault systems bounding the Chamo and Galana basins.

(3) Quaternary volcanic rocks they are exclusively restricted to the Chamo basin.

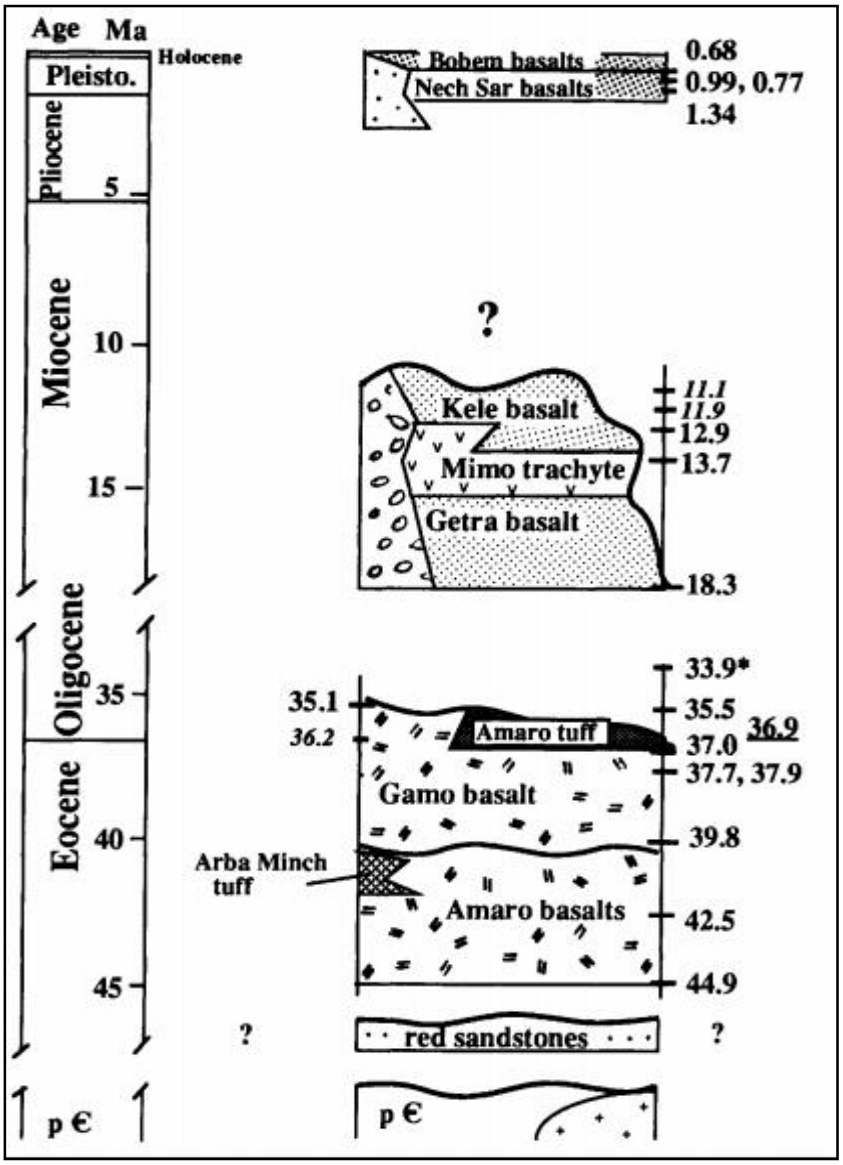

Figure1. 5 The stratigraphy of the southern Ethiopian rift basalts around Amaro (after Ebinger et al., 1993)

Chapter three

3. Methodology

3.1. Methodology

Within fourteen days spent in the field, fresh samples representing variations and different episodic flows were collected, lithologes are described both in outcrop and hand specimen level together with GPs location measurement and photograph. Among the collected samples based on their representativeness of the variation 15 samples for thin section and 10 samples for geochemistry were selected. For the thin section preparation the selected 15 samples were sent to the Geological Survey of Ethiopia Central Geological Laboratory and 10 samples were sent abroad through ALS lab in Addis Ababa to Ireland for the whole rock chemistry.

3.1.1. Sample analysis and description

The description of the thin section was carried out using the transmitted light microscope in Addis Ababa University laboratory. Thus identification of major rock forming minerals was done. The result of geochemical analysis was interpreted using diagrams for major, trace and base metals.

3.1.2. Analytical method

The whole rock analysis have been conducted at Analytical Testing Service (ALS, Ireland), by ICP-AES and ICP-MS where LOI determined by WST-SEQ instrument by heating 2g sample at 1000C and measuring loss of the weight. Major elements were analyzed by ICP-AES after four acid digestion and trace elements including REE elements were analyzed by ICP-MS after lithium borate fusion and four acid digestion. Analytical precision are estimated at 2% for major elements and at 5% for trace element concentration above 20ppm and 10% for trace element concentration below 20 ppm. The detection capacity of the methods for major elements is > 0.1% and for trace elements >0.1ppm except Cr and V which is >10ppm and >5ppm respectively.

Chapter four

4. Results

4.1. Stratigraphy and volcanology

Gidole horst consists of volcanic rocks of basalts and associated felsic rocks. It has ~ 1440m thickness with an episodic eruptions laying palaeosol between the successive eruptions. The recognized unites and their stratigraphic section is shown on figure 4.2. Generally, four volcanic stratigraphic units are named according their position from bottom to the top.

4.1.1. Lower basalts

The lower basalts are the first flood basalt lying at base of the horst over the metamorphic basement where it is exposed (e.g. around Gato) and are overlain by felsic tuff. This unit correlated with Amaro basalt (Levitte et al., 1974) and Ebinger et al. 1993 mapped some part of the study area in the eastern side with the Gamo-Amaro basalts. Approximately 305m thick of this basalt has 9 to 11episodic eruptions on the Eastern side of the horst along the road from Holte to the Gidole. Since it is the older rocks, they are highly weathered and less fresh compared to the successive eruptions. The lower flows are generally medium-grained, olivine-phyric with some with feldspar phenocrysts. Whereas the later flows are relatively fine grained and form less columnar joints around Gebele Beno.

Figure 4. 1 photographs of lower basalts showing A) episodic eruptions with little palaeosol at Pakayo B) the columnar joints around Pakayo

4.1.2. Felsic tuff (Gebele Beno tuff)

According to Ebinger et al. (2000) on the stratigraphy of Gamo-Gidole horst the felsic tuff of the study area were known as Gebele Beno tuff. This tuff uncomfortably overlays the lower

basalt and consists of the lower welded ignimbrite and the upper unwelded tuff. It is ~32m thick where the thicknesses vary to South of the Gebele Beno and terminate around Gato. The lower ignimbrite is light grey, well bedded and consists of a welded clasts and phenocrysts of sanidine. The upper tuff is soft, white and slightly gives efferevent reaction when treated by HCl. This indicates the presence of calcite in the rock and is possibly a result of water. It is related with the development of the rift basin in the early to middle Miocene time contemporaneous with the volcanic eruptions (Giday Woldegabriel et al 1991). The upper part of the tuff is highly weathered with variegated color of red and light grey indicating an oxidation of iron.

Figure 4. 2 a photograph showing the felsic tuff unite around Pakayo with lower ignimbrite and upper unweldded tuff.

4.1.3. Middle basalts

Middle basalts are the second phase of basaltic eruptions lying over the felsic tuff. This unit is aphyric and well known by its well-developed columnar joints particularly at the upper flows around Tare and hence, is a tool for differentiating this unit from the lower basalt, where felsic

tuff is absent. It has ~109m thickness with 5 to 6 episodic flows and is relatively fresh compared with the lower basalt.

Figure 4. 3 a photograph showing the columnar joints in the middle basalts around Tare

4.1.4. Trachyte

This unit does not cover a large area as felsic tuff and is well exposed around Himbro overlain by mudstone. It has an approximate thickness of 25m and form thin lenticular shape. It is fine-grained with a trachytic texture and has light grey color. The formation of mudstone indicates the presence of hiatus between this unit and the upper basalt.

Figure 4. 4 a photograph showing A) the trachyte around Himbro B) the highly weathered trachyte overlain by the mudstone near Tare

4.1.5. Upper basalts

These basalts are the last phase of eruption in among the rocks of Gidole horst. It has an approximate thickness of 525m with > 6 episodic eruptions. Since the upper flows of this basalt fall in sub-tropical (locally called Woinadega) climate condition of the area with high vegetation cover, they suffered a high alteration and even forming bentonite at the top of the area. Samples from these flows are not included.

Figure 4.5 a photograph showing an outcrop of upper basalt over the highly weathered trachyte unit near Tare

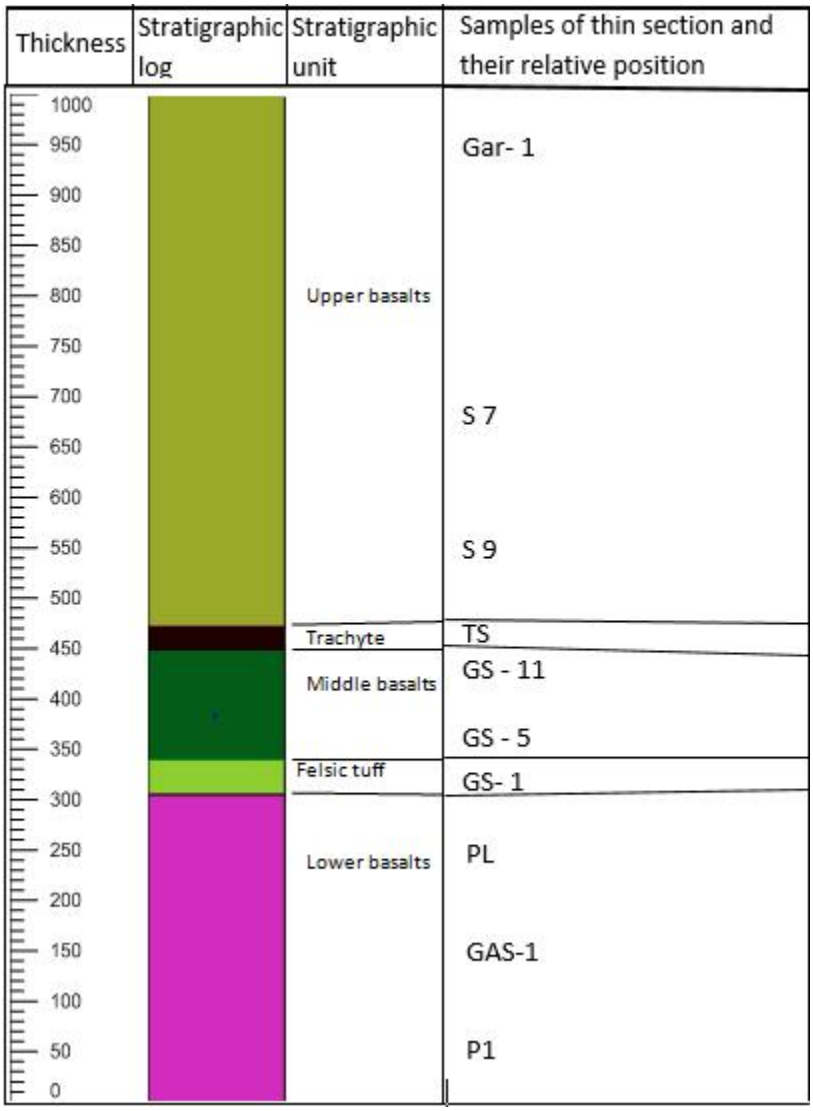

Figure 4.6. The stratigraphic log of the Gidole horst from Chamo basin side

Tectonic interpretation

Major faults are included in the Figure 4.7 Geological maps of the Gidole horst. Gidole horst is asymmetric; it is steep faulted on the western side and forms step up normal faults on its eastern side. The eastern side starting from Chamo basin marks a total displacement of 1000m with three step-up normal faults. Most faults orient in the North-south direction parallel to the main Ethiopian rift structures. However some faults orient at an angle to the N-S orienting faults terminates further propagation of the structures. More marginal step faults along the eastern side of the horst appear inactive. Recently also faulting occurred in Gidole town at angle to the rifting.

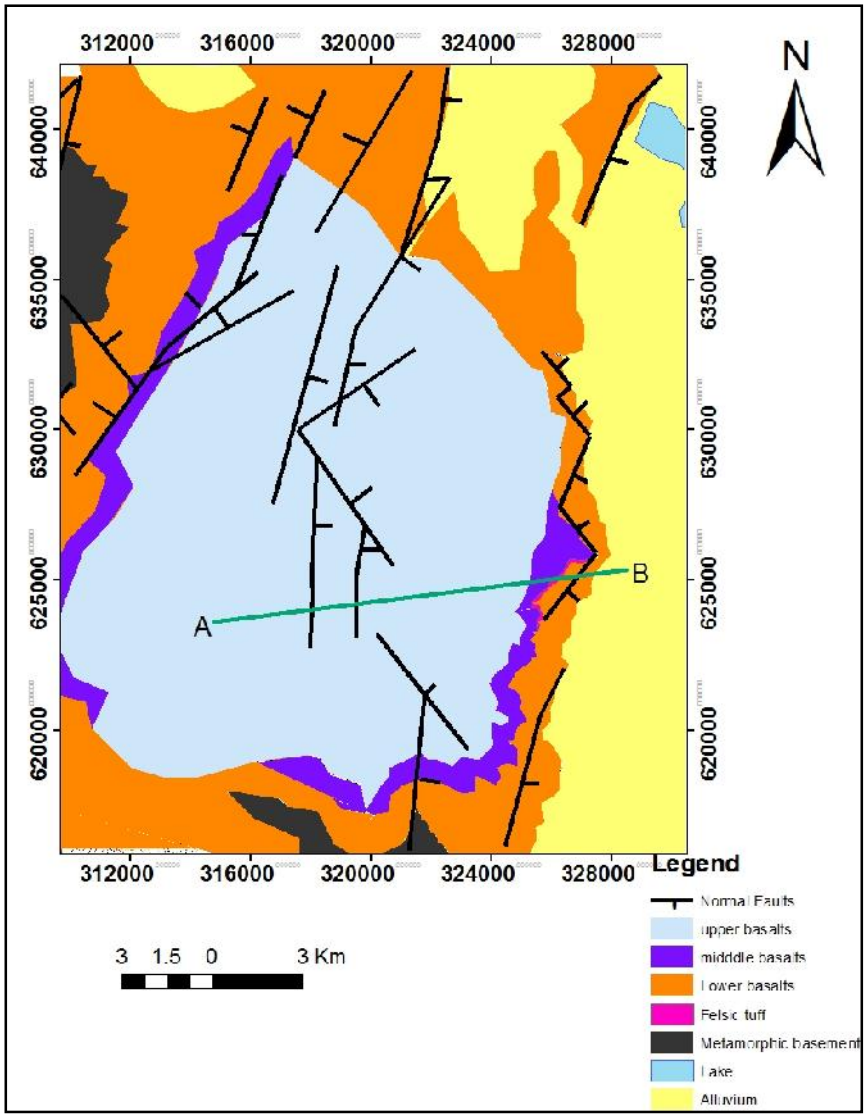

Figure 4. 7 Geological map of the study area (after Davidson A, 1983)

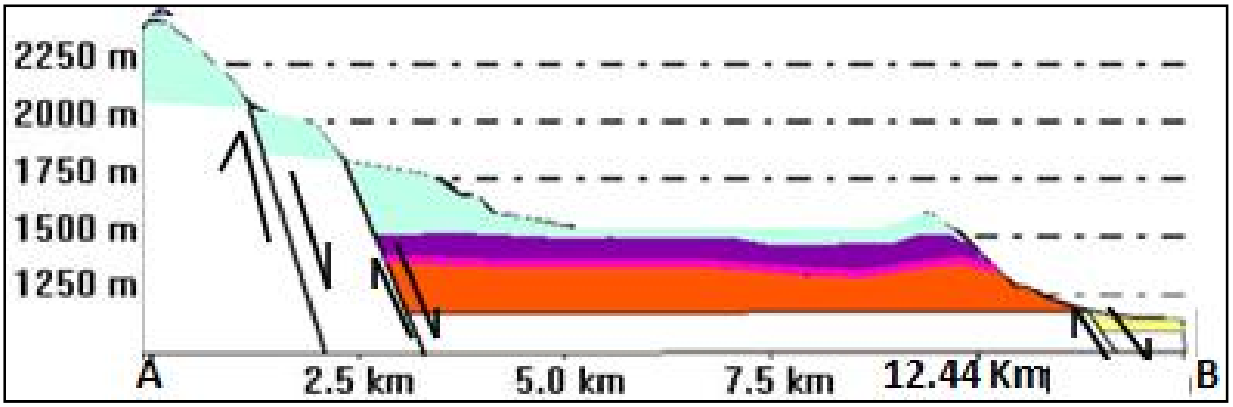

Figure 4. 8 The geological cross section of the Gidole horst from eastern side (symbols are the same with Geological map)

4.2. Petrography

4.2.1. Olivine-plag-phyric basalts

The lower basalts of the lower flows (e.g. GAS-1, GAS-3, P1 and PS-3) contain olivine and plagioclase phenocrysts and, with micro phenocrysts of plagioclase, olivine and pyroxene (fig 4.2.1). The ground mass is composed of the same minerals together with opaque mineral (roughly rectangular crystals probably magnetite). Olivine is altered to iddingsite and its proportion and alteration decreases toward the upper basalts where it is roughly altered along its rims and, plagioclase dominates. The lower most basalt (GAS-1) contains more olivine with plagioclase with occasional 2-3mm clinopyroxene forming ophitic texture where the oikocryst pyroxene encloses a lath shaped plagioclase. The plagioclase in these flows is lath shaped and show a preferential orientation, which may have resulted from flow of magma before solidification. Some plagioclase show normal compositional zoning and oscillatory zoning occurs in the plagioclase phenocrysts. While the upper flows are aphyric basalts lacking a phenocrysts of either plagioclase or olivine but the lath shaped plagioclase is dominant.

4.2.2 Aphyric basalts

The upper flows of lower basalts, the middle basalts and upper basalts are generally fine grained with sub-trachy texture. They contain micro-phenocrysts of plagioclase, pyroxene and olivine. The upper flows of the lower basalts (Pl) are relatively coarser than the middle and upper basalts. In the middle basalts (GS-5, GS-11 and GAS-6), micro-phenocrysts of plagioclase are a little oriented, inter-grown with opaque, pyroxene and olivine. The opaque proportions in those basalts are high and relatively larger compared with the others. The upper basalts (GS-9, GS-7, S-10 and Gar-1) contain microphenocrysts of plagioclase, pyroxene and opaque with the groundmass of the same minerals. S-7 and GS-10 are very fine grained with the lath shaped plagioclase.

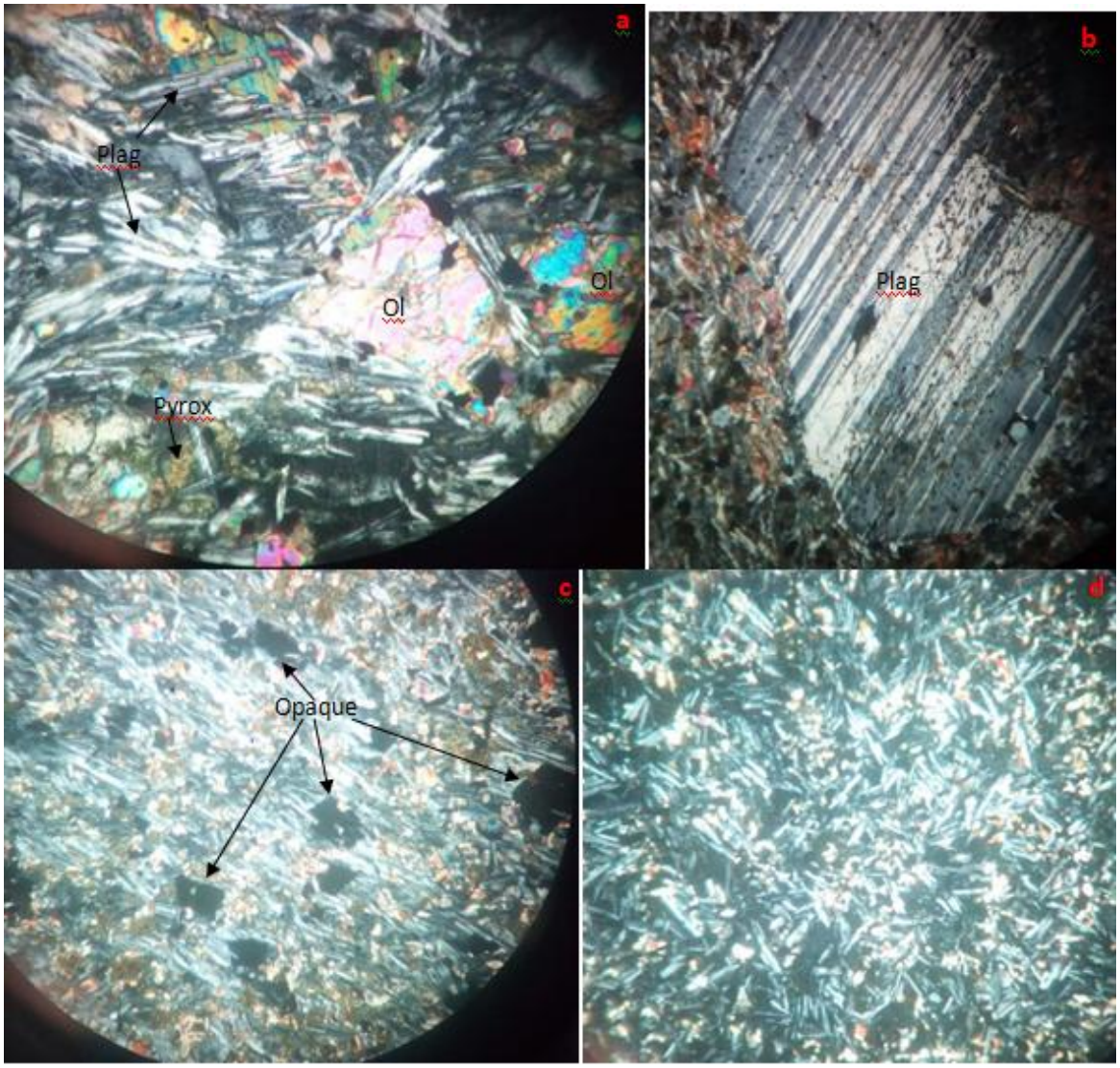

Figure 4.9. A photomicrography showing a) the phenocryst of early formed mineral olivine in the lower basalts of the lower flows (10 X). b) The phenocryst of plagioclase with polysynthetic twining (4X). c) The large opaque minerals in the middle basalts d) the upper basalts

4.2.3. Felsic tuff

The ignimbrite contains euhedral to subhedral phenocrysts of volcanic glass, sanidine, and quartz embedded in fine-grained groundmass of feldspar and biotite. The phenocrysts and ground mass are oriented to the same direction indicating the stress direction during the formation these rocks. Sanidine sometimes shows a simple contact twin and has a poikilitic texture enclosing the rock fragments. The felsic tuff samples contain volcanic fragments, feldspar and free quartz.

4.2.2. Trachyte

Trachyte is very fine grained with trachytic texture defined by <1mm long, aligned plagioclase lath. It contains plagioclase, amphibole and opaque minerals. The proportion of plagioclase is higher than the remaining minerals.

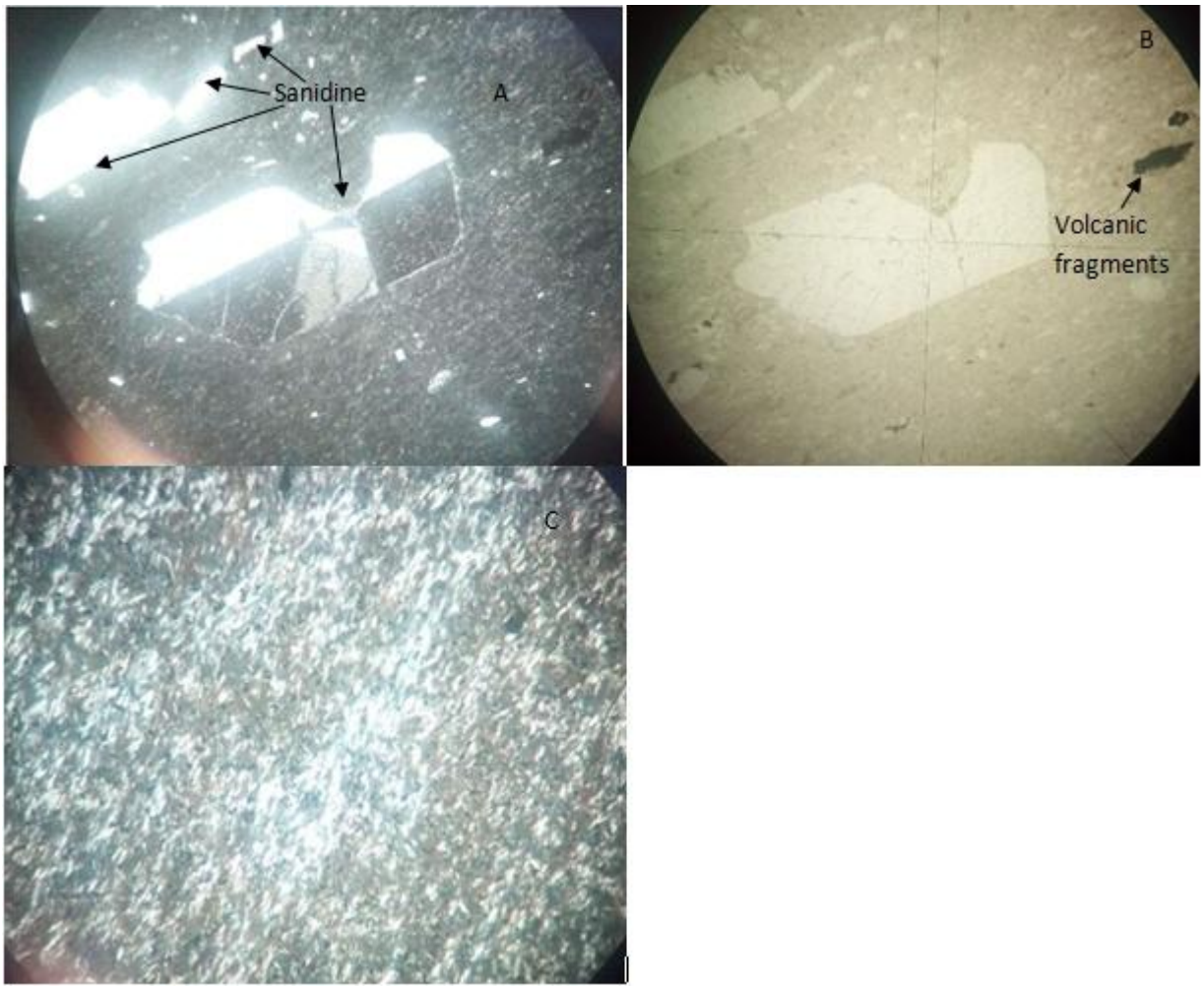

Figure 4.10. A Photomicrograph showing A) Sanidine minerals of varying size and some with simple contact twining in the ignimbrite within volcanic fragments. B) The Plane polarized view of the ignimbrite (4X) C) The trachyte with trachytic texture (10X).

4.3. Geochemistry

A reported on the major and trace element data for the selected 10 samples are below on table1.1. Accordingly, the total of major oxides including loss on ignition (LOI) fall between 98.49 and 100.65 suggests the analysis is good. The loss of index is good for basaltic rocks except the older basalts (e.g. P-1, PL and GAS-1) that have higher loss of index than the middle and upper basalts which indicate the probability of an alteration with water. The major element data have been recalculated to 100% on volatile freebase for geochemical classification. Iron oxide is the total iron and expressed as Fe_2O_3.

4.3.1. Major element

The basaltic rocks and associated rhyolite samples analyzed for their major oxide table 1.1 have a range of SiO_2 content from 45.76 to 76wt percentage. This SiO_2 content in basaltic rocks does not show an appreciable range and hence the lower and middle basalts are intermixed, while the two samples of the upper basalt are well differentiated among the rest of basalts having high SiO_2 content. The MgO have a wide range from 0.19 to 7.62wt % indicates there was a fractionation among the basalts and their derivatives. The lower value of the upper limit of the MgO suggests the older rocks also undergone a fractionation and are not a primary magma. The Al_2O_3 content have a range from 11.06 to 17.93wtpercentage. These ranges were obtained from felsic rocks while the basaltic rocks show a limited range of Al_2O_3 content (13.6 to 15.4wt %). Total iron oxide (expressed asFe_2O_3) content is less variable for the basaltic rocks (13.64 to 15.9wt %) where the felsic rockshaveFe_2O_3 content (5.56 and 3.92wt %). The rocks have a wide range CaO between 0.45-9.38wt percent. They also have a range for Na_2O and K_2O between 2.63-5.41 and 0.71-3.55wt percentage respectively and, total alkaline content (Na_2O + K_2O) ranges from 3.77 to 8.9wt percentage. TiO_2 content have a range from 0.41 to 3.44wt percentage where P_2O_5 content has a low value (<0.71wt %) except for the S 7 sample which is 1.16 wt percentage.

Table 1.1 chemical analysis of the selected samples where Major and minor oxides expressed in wt% and trace elements in ppm

	Lower basalts			**Middle basalts**		**Upper basalts**			**Trachyte**	**Rhyolite**
Oxides %	P1	GAS-3	PL	GS- 5	GS-11	Gar-1	S 9	S 7	TS	GS-1
SiO_2	45.3	45.3	46.3	46.3	47.1	47.9	49.2	49	61.7	70.8
TiO_2	2.09	2.3	3.37	3.44	2.77	3.41	2.88	3.17	1.42	0.41

Al_2O_3	15.1	15.4	14.85	13.85	13.9	13.6	13.85	13.6	17.7	10.3
Fe_2O_3	13.05	13.4	14.85	16.1	14.15	15.65	14	14.5	3.87	5.18
MnO	0.17	0.19	0.19	0.21	0.19	0.24	0.2	0.22	0.06	0.09
MgO	6.82	7.38	4.71	4.65	5.22	4.64	4.27	3.52	0.44	0.18
CaO	8.29	8.67	8.03	8.99	9.11	8.96	8.24	7.7	3.84	0.42
Na_2O	2.95	2.96	3.54	3.42	3.35	3.48	3.55	3.42	5.34	2.45
K_2O	0.82	0.69	1.29	0.84	0.91	1.12	1.42	1.7	3.45	3.31
P_2O_5	0.41	0.43	0.6	0.47	0.4	0.59	0.49	1.14	0.7	0.02
Cr_2O_3	0.022	0.019	0.005	0.002	0.009	0.004	0.006	0.002	0.002	0.003
SrO	0.1	0.05	0.05	0.05	0.04	0.05	0.05	0.05	0.08	<0.01
BaO	0.23	0.08	0.06	0.03	0.03	0.04	0.05	0.06	0.14	<0.01
LOI	3.9	2.52	2.8	0.85	1.61	0.3	0.28	1.66	1.14	7.2
Total	99.25	99.39	100.6	99.2	98.79	99.98	98.5	99.74	99.88	100.36

Trace element (ppm)	**Lower basalts**			**Middle Basalts**		**Upper basalts**			**Trachyte**	**Rhyolite**
	P1	GA S-3	PL	GS-5	GS-11	Gar-1	S 9	S 7	TS	GS-1
Sc	24	25	20	25	29	27	26	23	10	2
V	294	276	294	358	339	347	345	161	19	<5
Cr	150	120	30	10	50	20	40	10	10	20
Co	50	50	47	54	49	44	44	32	4	3
Ni	112	96	52	35	30	19	17	6	<1	2
Cu	50	47	34	138	89	53	38	25	1	2
Zn	104	111	139	154	126	144	155	161	125	294
Cs	0.09	0.11	0.07	0.23	0.13	0.19	0.38	0.5	0.69	1.42
Ga	20.4	20.5	24.6	24.7	22.3	24.7	24.2	24.6	28.2	36.2
Rb	11.8	10.6	20	19.8	13.9	19.8	28.9	37.9	63.7	154.5
Sr	1050	509	468	439	434	503	547	484	764	17
Y	25.6	25.9	34	31.9	28.1	33.9	33.8	47	38.3	153
Zr	127	141	268	252	187	232	254	320	581	1280
Nb	12.5	16.3	27.1	34.9	26.1	32	37.5	40	111	105
Ba	2100	696	501	285	299	375	509	486	1270	35.1
La	17.2	18.1	34.1	34.1	27.4	34.1	41.1	52	79.9	167
Ce	35.6	38.1	71.6	69.9	55.9	70.3	82	105.5	132	305
Pr	4.83	5.21	9.28	8.71	7.18	9.26	10.2	13.2	18.25	35.9
Nd	22.1	22.6	40.5	37.5	31.2	40	41.7	59.3	72.4	141.5
Sm	5.59	5.81	9.34	8.19	6.95	8.97	8.94	12.8	13.25	27.8
Eu	1.98	2.22	2.7	2.78	2.5	2.79	2.77	4.03	4.56	3.12
Gd	5.24	6.12	8.49	8.19	7.31	8.46	8.27	12.65	10.45	25.5
Tb	0.85	0.89	1.22	1.19	1.02	1.24	1.16	1.77	1.44	4
Dy	4.91	4.98	6.57	6.47	5.6	6.71	6.49	10.2	7.96	23.6
Ho	0.99	0.97	1.34	1.27	1.11	1.35	1.27	1.9	1.56	5.09

Er	2.93	2.89	3.77	3.54	3	3.55	3.57	5.49	4.16	14.65
Tm	0.35	0.33	0.45	0.42	0.4	0.46	0.44	0.65	0.55	1.94
Yb	2.33	2.47	3.1	2.99	2.46	2.8	3.06	4.16	3.48	13.15
Lu	0.35	0.33	0.43	0.4	0.37	0.41	0.42	0.62	0.51	1.9
Hf	3.1	3.6	6.4	6.3	5	5.8	6.4	8.1	13.5	31.8
Ta	0.6	0.8	1.3	1.8	1.5	1.8	2.1	2.2	6.8	6
Pb	2	<2	2	4	4	4	6	3	4	29
Th	1.42	1.43	2.8	4.06	3.01	3.27	4.42	5.46	10.65	22
U	0.35	0.43	0.71	1.13	0.74	0.88	1.09	1.61	3.71	4.29

Figure 4.11 the TAS classification diagram, rocks from Gidole horst plot in to alkaline field near to sub-alkaline/tholeiitic and they are truly transitional basalts. The rhyolitic ignimbrite is the only rock that plot on the sub-alkaline field. This rock has high loss on ignition (LOI) and low Na_2O content suggests that the loss of sodium by deutetic process probably leaching by surface of the glass (Gezahegn Yirgue et al., 1999, Percerillo et al., 2003). The alternative classification of basalts Nb/Y versus Zr/Ti modified by pearce 1996 (not shown) plot the rhyolite on the alkaline rhyolite, which may supports its secondary alteration. On the TAS classification the rocks plot on the field of basalt, trachy-basalt, trachy-dacite/trachyte and rhyolite, missing intermediated rocks, like basaltic trachy-andesite and trachy andesite. This property is called bimodal composition, which is the characteristic of the East African rift system (e.g. Barker et al 1996b), and the plot on the alkaline to transitional basalt supports the rocks of the Ethiopian rift system.

The variation diagrams of Major oxides vs. MgO on Harker diagram (Figure 4.12) for the rocks of Gidole horst shows a smooth trend as MgO decreases and suggests that the rocks are genetically related at some fashion with the gap of SiO2 from 50.1 to 62.49wt percentage that is commonly called a Daly gap. The increase in K_2O and Na_2O with decreasing MgO concentration from lower basalts through the upper basalts to evolved rhyolites indicates they are not included in the fractionating minerals. Generally, from lower basalts to the middle basalts SiO_2 increases a little, Al_2O_3 decreases, and CaO and CaO/Al_2O_3 increases with decreasing MgO suggesting plagioclase and olivine is the dominant fractionating mineral over the pyroxene in the early phases of eruption. The little decrease of MgO and still decrease of Al2O3 from middle basalts to upper basalts with a decrease of CaO/Al_2O_3 indicate, pyroxene and plagioclase are the dominant fractionating minerals than olivine of the later lavas. Fe_2O_3 and

TiO_2 decrease from middle to upper basalts indicate they accumulate Fe-Ti oxides together with the fractionating minerals. However, P_2O_5show slight decrease from lower to the middle basalts with decreasing MgO suggests a little accumulation of apatite together with olivine and plagioclase in the lower basalts. A very High concentration of Al_2O_3, Na_2O in the trachyte and a rapid decrease in the rhyolitic rock suggests strong fractionation of sodic plagioclase. Classification of rhyolites and trachytes into comenditic and pantelleritic using Al_2O_3 versus total iron (Macdonald 1974) were classified the samples as comenditic trachyte and pantelleritic rhyolite.

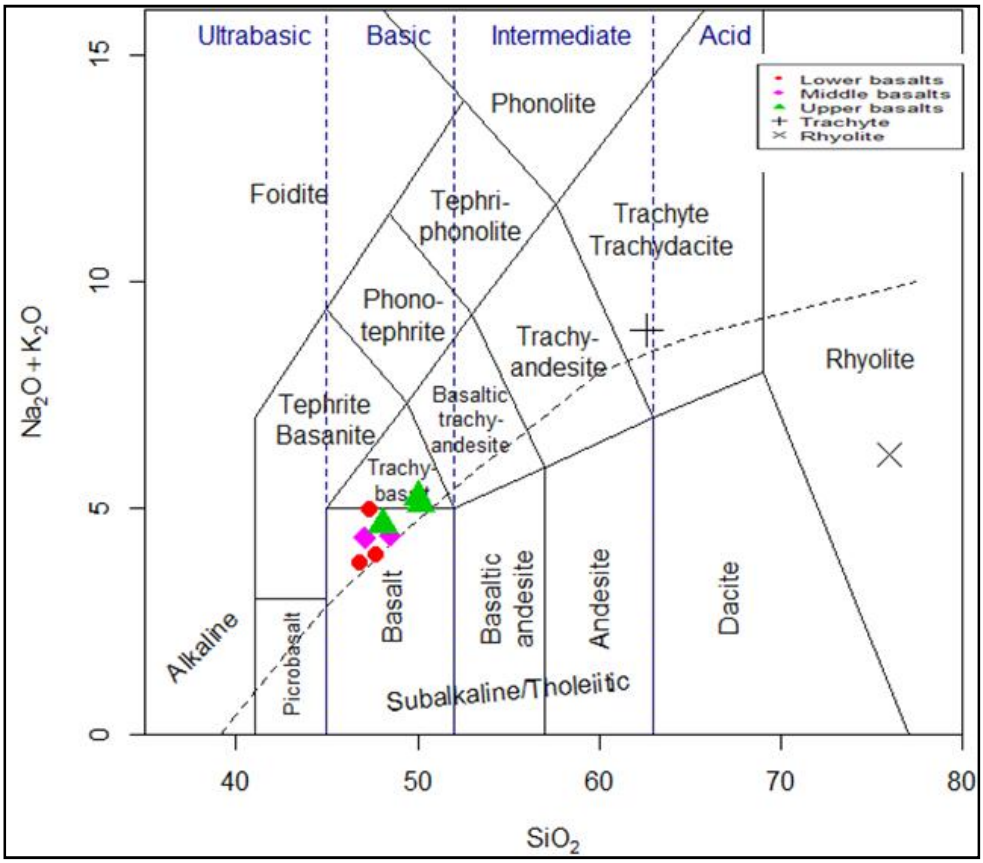

Figure 4. 11. Total alkaline silica diagram for the rocks of Gidole horst (Le bas et al. 1986) SiO_2 versus total alkaline silica. Alkaline-sub alkaline line division is from Irvine and Baragar (1971)

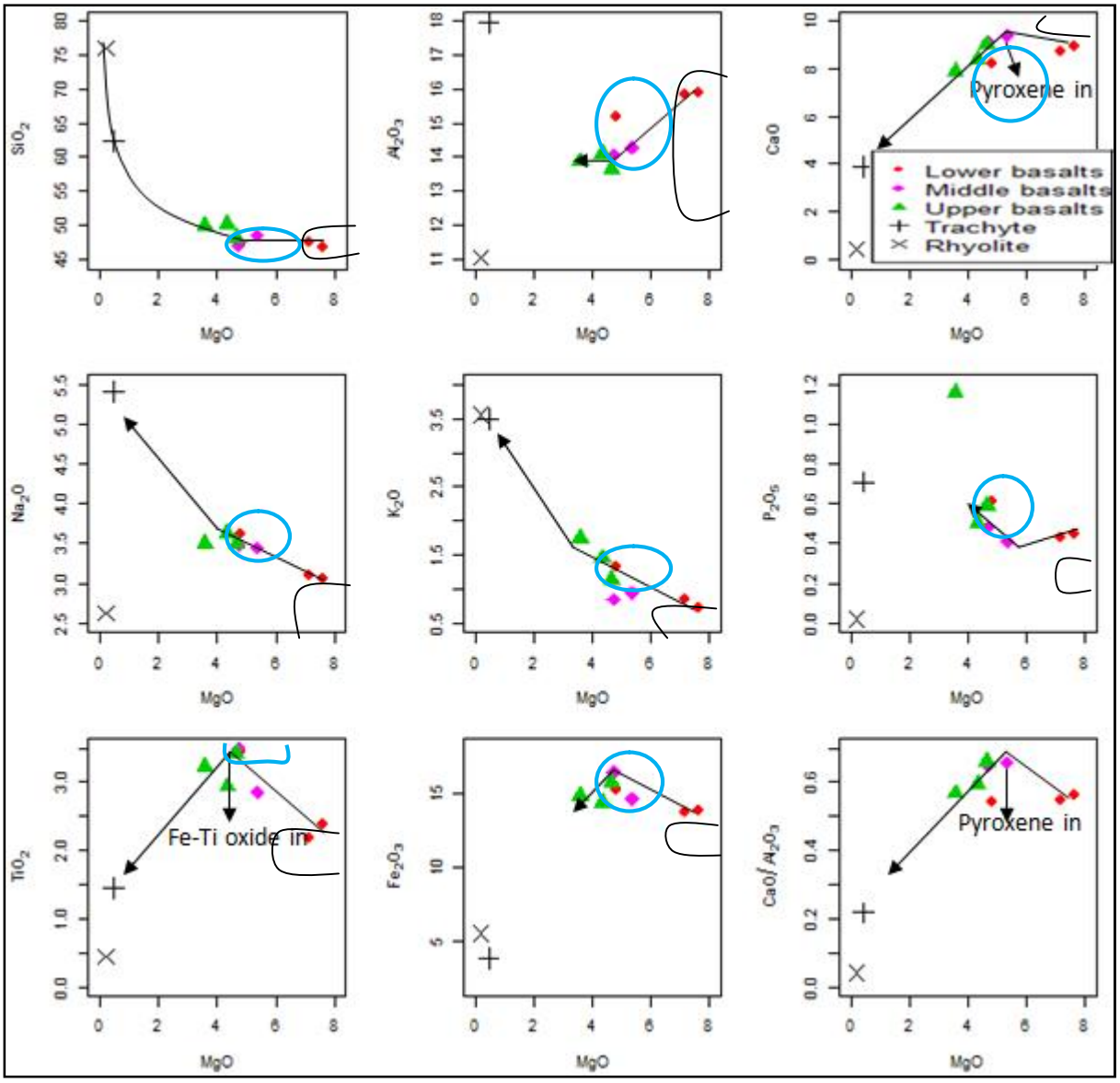

Figure 4.12. The variation diagrams of MgO versus Al_2O_3, CaO, MgO, Na_2O, K_2O, P_2O_5, TiO_2 and CaO/Al_2O_3, of the basaltic magma and associated rhyolites of Gidole horst. The blue circles represents the range of Gamo basalts and the black curve represent the field of Amaro basalt indicating there are samples with Mg above the range. The Getra – Kele basalt is not represented here since it covers wide range of Mg.

4.3.2. Trace element

The variation diagrams of trace elements are plotted against MgO for both compatible and incompatible elements. Thus, the plot of compatible transitional elements (Ni, Cr, Sc, Cu, Co and V) versus MgO shows a rapid decrease with decreasing MgO for the highly compatible elements Ni and Cr (fig 4.13). The rapid decrease of Ni concentration between the lower basalt

and middle basalt indicate the fractionation of olivine. Since they are compatible elements, they were incorporated into the early forming minerals such as olivine and, indicate the fractionation of those minerals that were verified by thin section as phenocrysts in the lower basalts. The slight decrease in the slope after middle basalts suggests the decrease and/or absence of those minerals. The other elements (Sc, Cu, Co and V) on the other hand show their higher concentration in the middle basalts than the lower basalts. This increase of those elements with decreasing MgO suggests pyroxene is the fractionation phase next to olivine and plagioclase.

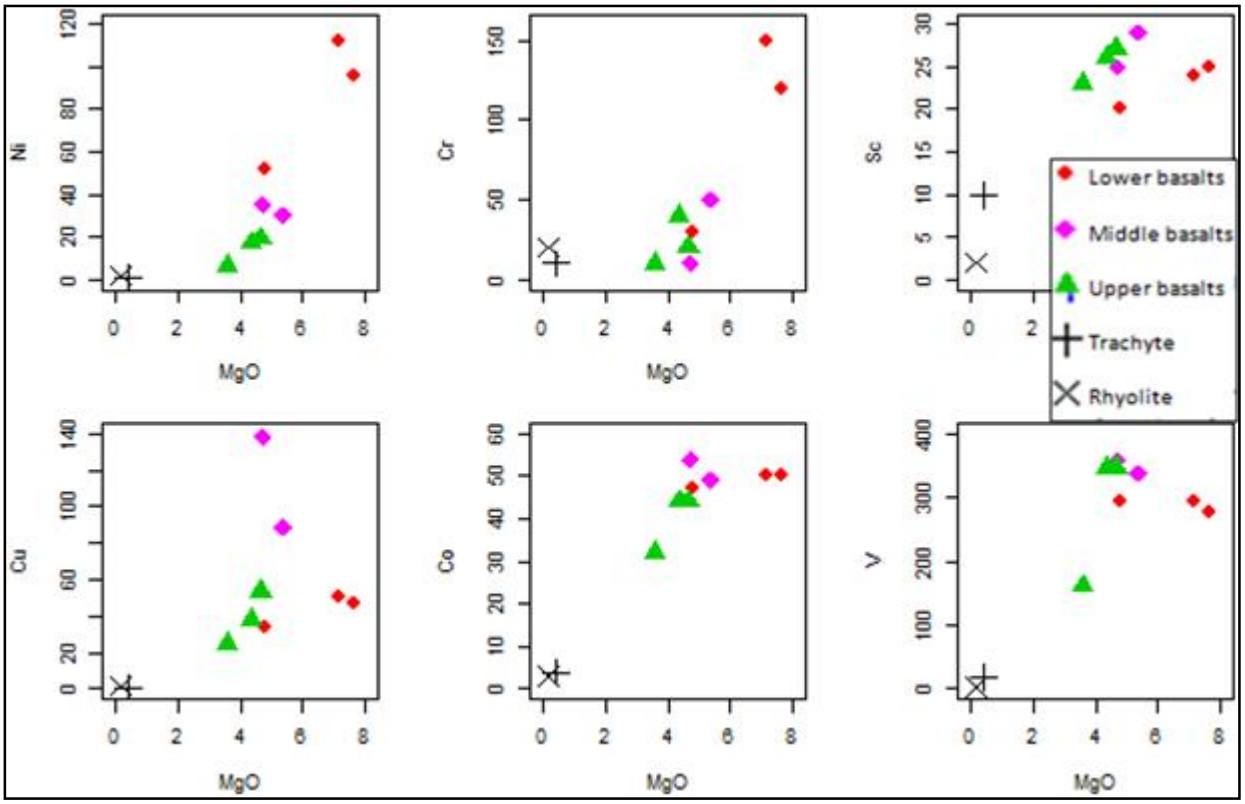

Figure 4.13. Plot of compatible transitional elements (Ni, Cr, Sc, Cu, Co, V) versus MgO of the volcanic rocks from Gidole horst

The variation diagram of incompatible element verses MgO (figure 4.14) show strong positive relationship from lower basalts to upper basalts and then to rhyolitic rocks except for the Ba and Sr concentration, which has a scatter plot. This relationship reveals the association of the rocks and their evolution trend. The Rb, Ce, La, Zr and Th have a strong relationship from lower basalts to the rhyolitic rocks with MgO suggesting fractional crystallization is the dominant processes that control the evolution of the magma. Similarly, Nb, Ta and U show a smooth trend within the basalts and nearly with trachyte whereas, rhyolitic ignimbrite have a lower values of

those elements. The relative lower concentration of Y observed in trachyte also seen in Pb element (not shown). Ba and Sr have a generally scatter plot with higher concentrations in lower basalts incorporated in early forming Ca-plagioclase (Wilson 2007) and very low concentrations in the ignimbritic rhyolite. The higher concentration of Ba and Sr in lower basalts may indicate the alteration or metasomatism since they are fluid immobile or, associated with the shallow level fractionation of plagioclase, which is the early forming mineral with olivine. These two elements are also highly depleted in the rhyolitic ignimbrite. The higher concentrations of barium in basaltic rocks in Ethiopian basalts were thought before by many authors (e.g. Jones 1976, hart et al 1989; George and Roger 2002). The basalts and the associated rhyolites have an elevated Zr/Hf ratio than the chondrite and primitive mantle (data from Sun and Mcdonough 1989)

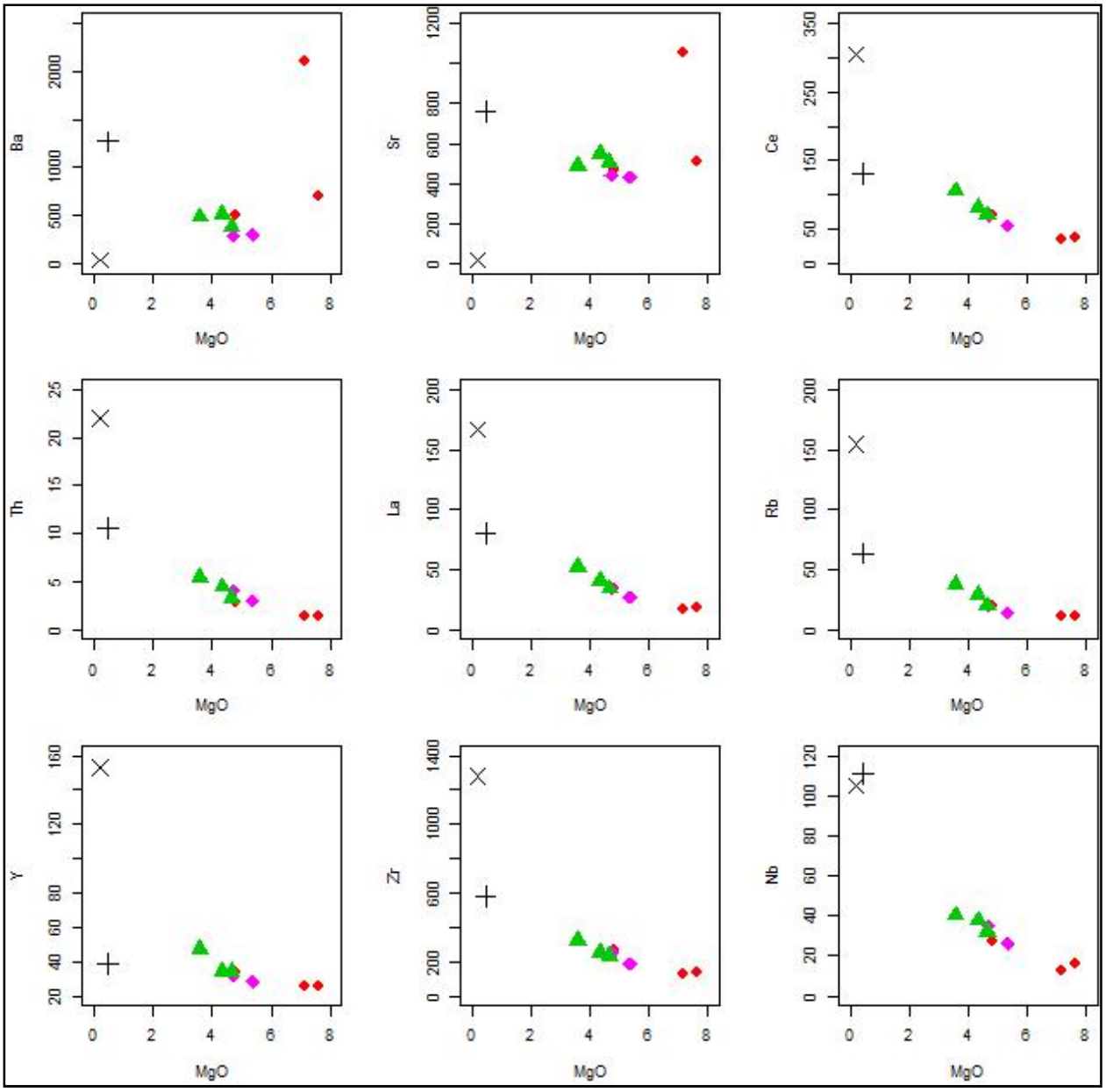

Figure 4.14. The plot of incompatible elements (HFSE and LILE) versus MgO of the volcanic rocks of Gidole horst

The spider diagram normalized to the primitive mantle (fig 4.15) is decreasing down ward from left to the right. All flow magmas (basalts and trachyte) have high concentration barium, which is related to Ethiopian basalts as, described in trace element. The basaltic rocks form a trough between Ba and La while among the basalts the lower basalts have a K peak in between Ba and La (i.e trough at Rb-Th and Nb-Ta), suggests, the contamination of magma with lower continental crust rocks (Cox &Hawkesworth 1985). Moreover, lower basalts also have peaks at

Sr and P indicating plagioclase and apatite fractionation. In contrast to the basalts, the felsic rocks (rhyolitic ignimbrite and trachyte) have a strong through at Ba, Sr, Ti and P indicating feldspar, apatite, and Fe-Ti oxide fractionation. Those troughs also observed in the felsic rocks of northern Ethiopia (e.g. Dereje et al., .2001) and Yemen (e.g. Baker et al., 1996b).

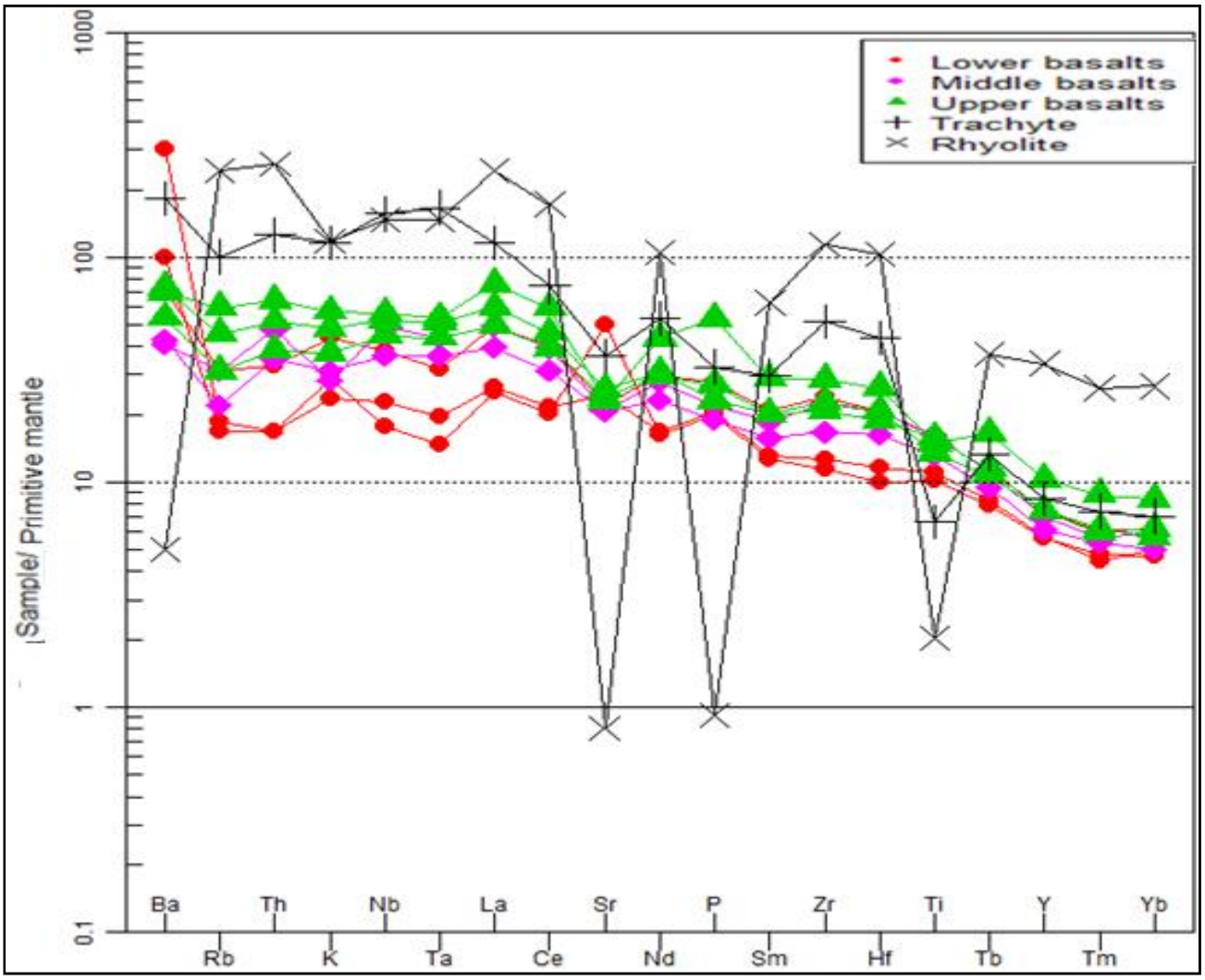

Figure 4.15. Primitive mantle normalized spider diagram showing trace element patterns of Gidole horst normalized to Sun and McDonough (1989)

4.3.3. REE element

The diagram of Chondrite-normalized REE elements (Fig 4.16) shows an enrichment of light REE and strong depletion of heavy REE compared to E-MORB they have different source, but have similar source with OIT. Therefore, they have a strong negative slope of REE and HREE with an exception of the rhyolite, which have shown slight negative slop and have negative Eu

anomaly. The negative Eu anomaly and very low concentrations of Ba and Sr in the rhyolitic ignimbrite suggests plagioclase fractionation in the early phase. The Chondrite-Normalized REE diagram of the samples is sub-parallel showing an increase of the slope from highly mafic (GS-1 and GAS-3) to trachyte (TS) and, is an indication of fractional crystallization subsequent to magma segregation from the source. The trachyte pattern mimics the trend of the basaltic rocks with slight variations while the rhyolitic ignimbrites have a different pattern especially in the high HREE.

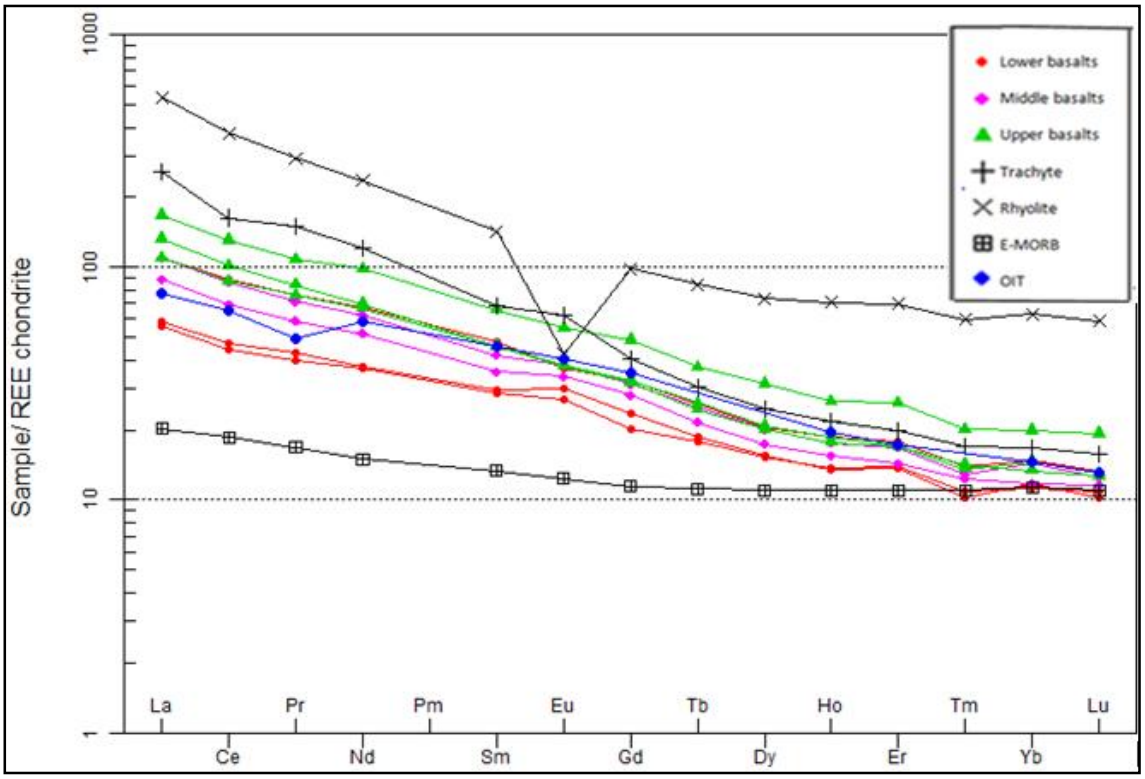

Figure 4.16. Chondrite normalized spider diagram showing the REE element patterns of the Gidole horst rocks (Boynton 1984): the basalts MORB and OIT data are from Sun and Mcdonough 1989 and Wilson 2007 respectively.

Chapter five

5. Discussion

To constrain petrogenesis and their source rocks of Gidole horst, samples are selected based on their freshness. However, the older rocks show an alteration, high loss of index and are generally less fresh compared to the later phases of eruption. As a result, most interpretation has been related to the HFS elements than LIL elements, since they are less susceptible to alteration and weathering. In a general sense, high LIL element indicates the enrichment either of the source or due to the alteration and / or alteration with the crust.

5.1. Petrogenesis of Gidole horst basalts

The pronounce bimodal composition of main Ethiopian rift rocks are reported by many authors (Baker 1996b, Peccerillo 2003;Dereje A. & Gibson A. 2009;Ronga et al.,2010) in the East African rift system. Similarly, rocks from the Gidole horst have showed a bimodal composition, missing intermediate rocks. It consists of more mafic lava flows and the flow and pyroclastic felsic lavas. The mafic lavas have three phases of basaltic eruption separated by the evolved products in the Gidole horst show a considerable differentiation from bottom to top. From thin section study, the lower basalts have olivine, plagioclase, pyroxene and opaque (roughly rectangular probably magnetite) minerals. The concentration of olivine decreases from lower to the upper while pyroxene increase and amphibole appears within the groundmass in the upper basalt. The fractionation sequence of Gidole horst would be olivine, plagioclase (which remain throughout the phase but change from Calcic to sodic), pyroxene, Fe-Oxide and amphibole.

5.1.1 Fractional crystallization

Based on the Mg#, MgO and Ni concentration the lower basalts have high Mg# ~55 and MgO ~7.5 compared to the upper basalts and laid within the range in the most primitive magma in the southern rift (George & Rogers, 2002). They have low MgO, Ni content, High Na_2O, and K_2O than the most primitive magma of Amaro basalts. However, the plot on the TAS classification, the lower basalt plots on the transitional field than the tholeiitic field as the Amaro basalts indicated by George and Rogers (2002), but Zr versus Nb plot (fig 4.17) and low TiO_2 concentration (fig 4.12) support they are from the same source with Amaro basalts rather than Gamo basalts. If this is true, the low value of MgO and CaO, and higher values of Na_2O and K_2O

in the lower basalts compared to the most primitive magma suggesting the magma itself experienced some degree of olivine fractionation en route to the surface. Due to this reason, the lower flows that are highly weathered around Gato (e.g. GAS-1) or, unexposed around Holte may have high Ni and magnesium content or, the lower values are similar with the main Ethiopian rift basalts (Dereje Ayalew et al., 2016). George and Rogers (2002) reported the lack of relationship between the Eocene Amaro basalts and the Miocene Getra-Kele basalts showing different sources. However, the later phases of Gidole horst have strong evolution trend from lower to the upper basalts on variation diagrams as well as on the spider plots with an exception of the upper phase of the lower basalt PL and the upper phase of upper basalt Gar-1 that plot with the middle basalts. Those three phases irrespective of different thickness show strong relationship rather than different source rock in contrast to the George and Rogers (2002) of the three eruptive phases. Therefore the three phases of Gidole horst basalts are only related with the first phase of eruptions Amaro and Gamo basalts between 45 and 35Ma.

Despite their low Ni and Mg# concentrations, the lower basalts of the Gidole horst plot with the older Amaro basalt rocks (figure 4.12) and suggest the lower basalt of the Gidole horst are the first phase of eruption (occurred in Eocene) equivalent to Amaro basalts. Thus, the strong correlation of the later phase with the lower basalts from Gidole horst including the rhyolitic rocks on the variation diagrams of major, trace element and spider diagrams indicate they share common source and formed by crystal fractionation from the lower basalt. Such fractionation will tend to increase incompatible elements from the primitive to the more evolved magmas without enter-element fractionation. The increase in incompatible elements and decrease in compatible elements were verified in the trace element variation diagrams and no marked inter element fractionation.

The variation diagrams of major oxide, trace elements and spider diagrams go hand in hand supporting crystal/liquid fractionation rather than different sources. On the major element data among the basalts (Fig 4.12), there is a change in the courses indicating the change in the fractionating minerals from lower basalts to the upper basalts. For example, the decrease in Al_2O_3, P_2O_5 with decreasing MgO from lower basalts and middle basalts suggests the fractionation of olivine, plagioclase and apatite in the lower basalts. The Al_2O_3 continue to decrease to the upper basalts, while P_2O_5 change its course and, instead Fe_2O_3, TiO_2 and CaO

start to decrease. This indicates the fractionation of olivine, pyroxene, plagioclase and Fe-Ti oxide that continue until the upper basalts. The fractionation of plagioclase to the early forming minerals is also common in OIT basalts (Wilison, 2007). Similarly, within the main Ethiopian rift olivine, clinopyroxene and plagioclase are the dominant silicate phases within the more mafic products (Trua et al., 1999; Rooney et al., 2007). However, the higher concentration of Sr in the lower basalt together with plagioclase fractionation indicates shallow level fractionation of plagioclase (Winter 2014). The fractionation of plagioclase after olivine suggested as high-pressure clino-pyroxene fractionation of an originally tholeiitic parent in the Gamo basalts (George and Rogers 2002).

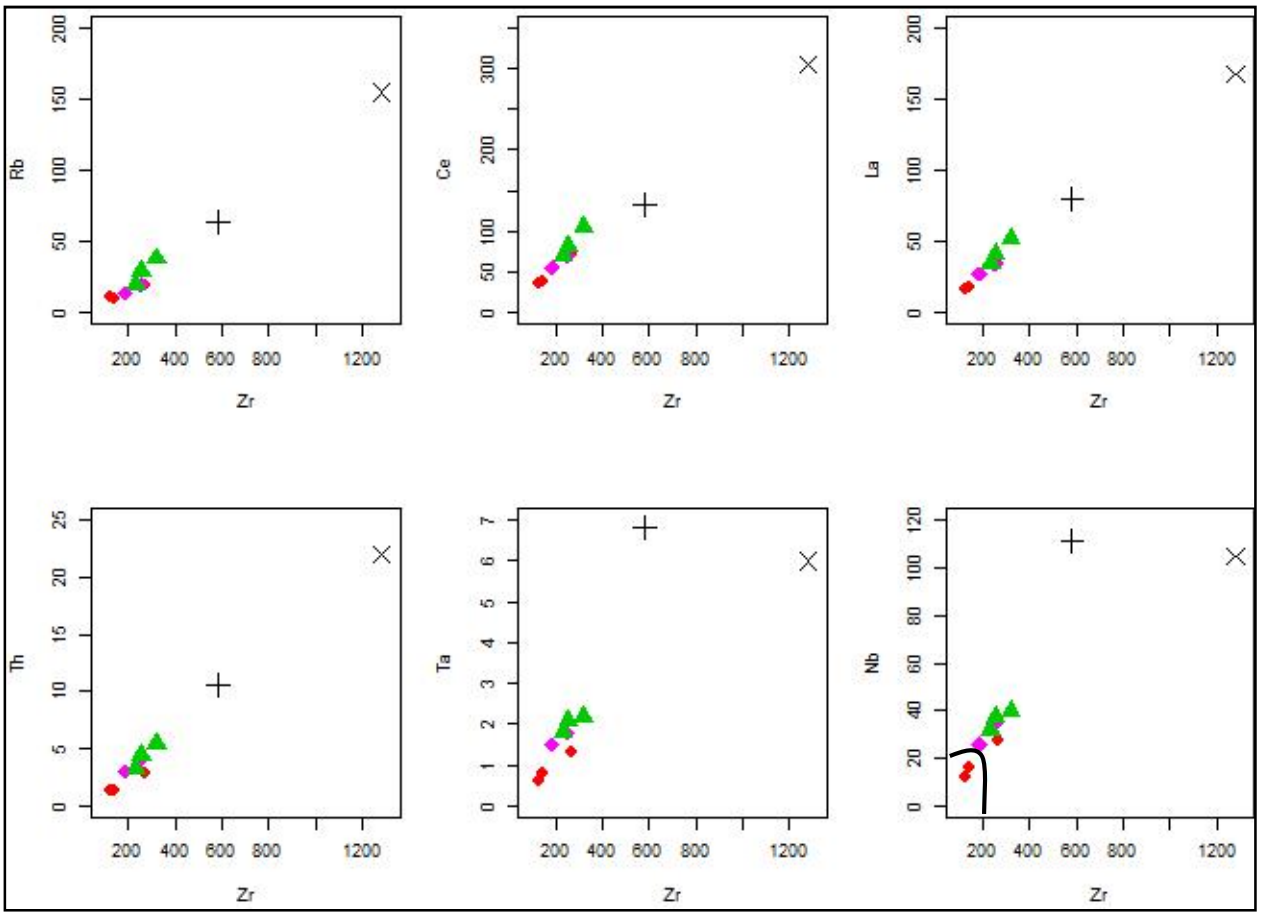

Figure 4.17. Variation diagram of incompatible elements versus highly incompatible element Zr element. The curves in the Nb versus Zr show the range of Amaro basalt (data from George and Rogers 2002) where they used to differentiate Amaro and Gamo basalts as well as Getra-Kele basalts. Here the Gidole lower basalt of lower basalts plots on the Amaro basalts field.

The trace element variation diagrams of volcanic rocks of Gidole horst reveal the co-genetic relationship of the rocks. On the variation diagram of compatible transitional elements versus MgO(fig 4.13) there is an abrupt drop in Ni from lower to the middle basalts suggesting the fractionation of Olivine, as fractionation produce nearly vertical line than partial melting (Winter 2014). Chromium also has similar Pattern as Ni and suggesting Cr-rich spinel with some pyroxene fractionated as Cr enter olivine slightly but strongly fractionate into pyroxene.

Moreover, the variation diagrams of incompatible versus Zr (fig 4.17) generally show the increase of the incompatible elements with the increase of Zr. These relationships result a nearly constant ratio between those elements and is due to Fractional crystallization. The constant ratio La/Hf and Zr/Ce reported before by Barbari et al (1975) as fractionation –controlled the evolution support the crystal fractionation that has occurred between the rocks including the more evolved products. Similarly, Hofmann (2003) suggested that variations in Th/U, Nb/U, Nb/La, Ba/Th and Pb/Nd, should reflect source differences rather than evolution and, therefore there is no much more variation among the samples. Rather they tend to have much close ratios indicating the fact that fractionation is the dominant process that produced the evolved rocks from the lower basalts. In addition, the ratio of the two similar incompatible elements Sm/Hf of the samples is close to the chondrite ~1.45. Indeed, in the absence of radiogenic isotope data to confirm liquid line of descent, consistence of incompatible element ratio provides a strong evidence for the crystal fractionation with a limited contamination. However, the ratio of Nb/U and Ce/Pb, which is thought to be constant for MORB and OIB (Hofmann and White 1983, Hofmann et al 1986, Newsom et al 1986) is lower than the constant value and suggests the contamination of magma with the crust.

The crystal fractionation of early phase minerals (olivine, plagioclase, clinopyroxene and magnetite) never affect the primary shape of the REE pattern, instead increases the total REE content of more evolved products(Wilson, 2007, Winter 2014). This is because REE are incompatible with respect to the major phases crystallizing and are increasingly concentrated in the more evolved liquids. Therefore, the sub parallel pattern produced by the basalts of Gidole horst from lower basalts to the rhyolites with a little/no inter-element fractionation indicates the latter rocks are formed by crystal fractionation (Wilson2007). As a result, the primary shape of the REE pattern from lower basalts is unaffected, while absolute abundances of the elements

increase. This is due to the incompatibility of REE with respect to the early forming minerals and tends to concentrate in the residual liquid.

The spider diagram normalized to the primitive mantle (Fig 4.15) has a peak in Ba for all basaltic rocks. The relative high concentrations of Ba and Sr in the lower basalts indicate the shallow level fractional crystallization of plagioclase (Wilson 2007). The trough at Th and Rb combined with one at Nb-Ta especially in the lower basalts may suggest contamination of magma by continental crustal rocks (Cox and Hackswarth 1985, Wilson 2007). The fractional crystallization combined with assimilation also reported by Baker et al (1996b) in the Yemen rocks.

5.1.2. Crystal Contamination

A trough at Th and Rb and, at Nb-Ta combined with the peaks at Sr and Ba in the lower basalts from mantle-normalized diagram (figure 4.15) suggests contamination of magma by lower continental rocks (Wilson 2007) during magma ascent to the surface. Amphibole bearing source will produce high Ba and low K concentrations (Dereje Ayalew et al., 2016). Similarly, melts derived from readily fusible metasomatized sub-continental lithosphere are thought to be enriched in Ba and depletion in K relative to LILE (Ce, Rb) and to have elevated LREE abundances on mantle-normalized incompatible elements plot (Furman 2007, Dereje Ayalew et al., 2006b;Dereje and Gibson 2009). However, the rocks of Gidole horst don't show K depletion on the spider diagram normalized to the primitive mantle. Rather the lower basalts show an enrichment K, indicates the rocks are crustal contaminated specifically with the lower crusts. These higher value of k may arise from their high loss of index for the lower basalts (>2.5) as K is derived from K_2O recalculated to 100% after volatile freebase.

Lower Ce/Pb is typical of crustal contamination (e.g. Furman 2007; Rooney 2010), and the volcanic rocks of Gidole horst have lower Ce/Pb and lower Nb/U (fig 4.18) with some plots above the Ce/Pb. The High La/Nb and Ba/Nb together with low Ce/ Pb in the more evolved lavas used as an evidence for crustal contamination during crystal fractionation (Dereje & Gibson, 2009). Even though the volcanic rocks of Gidole horst have higher Ba/Nb and Low Ce/Pb (fig 4.12), they have a ratio of La/Nb (not shown) similar to OIT (data from Wilson 2004) which is higher than the MORB and OIB (data from (Sun & McDonough, 1989)) indicating similar

source with OIT and later modification by lower curst. However, some samples the upper phase of lower basalt (PL), middle phase of the upper basalt (S 7) and trachyte (TS) plot above the Ce/Pb and those samples show low Pb concentration and need better justification using radiogenic isotope data.

Figure 4.19 shows the spider diagram normalized to OIT with mobile elements on the left side and less mobile on the right side with increasing incompatibility. The Gidole horst rocks show a seesaw shape on the fluid mobile elements side and have a less effect on the less mobile element side. Compared to OIT basalt they have an enrichment of Ba and Th and depletion of Ta. This enrichment of barium is obvious in Ethiopian rift system as is reported by many authors (e.g. Jones 1976; Hart et al., 1989; George and Rogers 2002; Dereje Ayalew et al 20016).

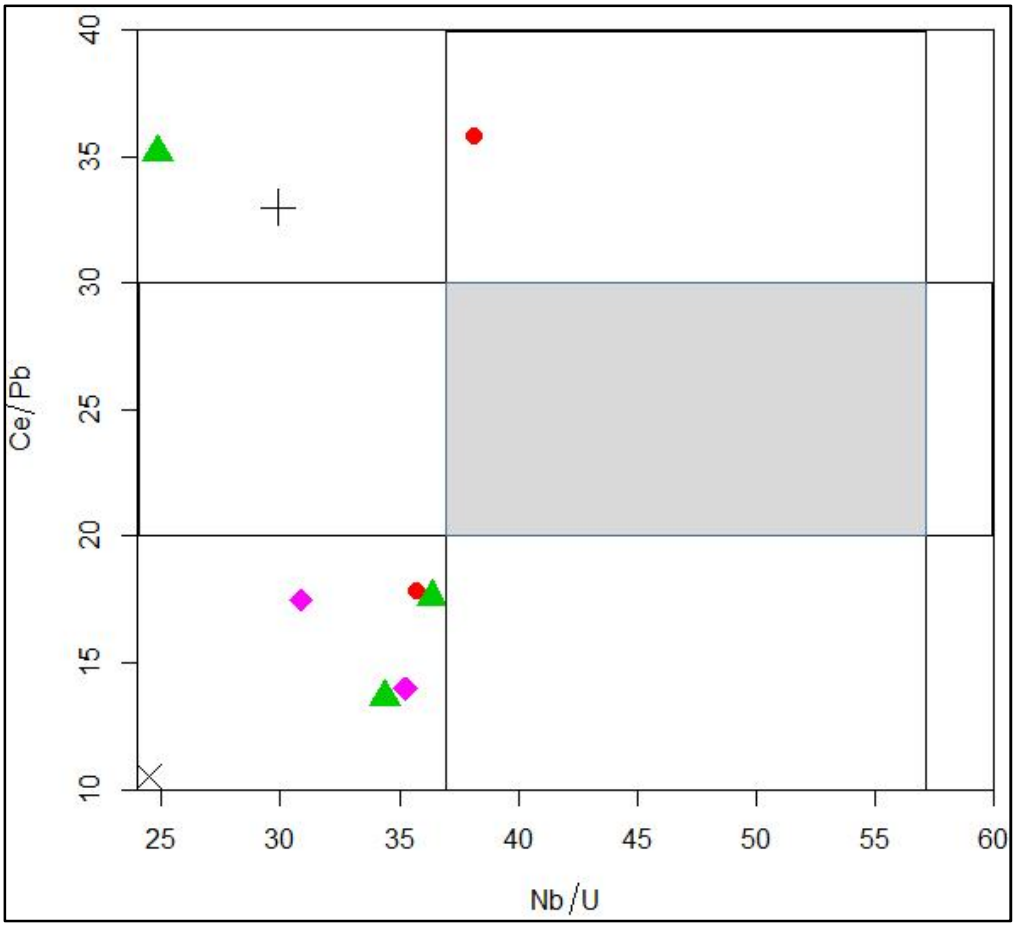

Figure 4.18. The variation diagram Ce/Pb versus Nb/U for Gidole volcanic rocks. Most samples plot on the low Ce/Pb and low Nb/U indicating the existence of crustal contamination but from lower basalt PL, upper basalts S 7 and trachyte plot above Ce/Pb.

The enrichment of Ba and depletion of Ta indicate the involvement of sub continental lithosphere (Pearce 1983; Wilson 2007) for the rocks come from the mantle. Therefore, Th/Yb versus Ta/ Yb as indicated by Pearce (1983), the uncontaminated samples and MORB should define a unity, as mantle enrichment concentrate both Th and Ta equally. Similarly, partial melting and fractional crystallization have a less pronounced effect on the variations of these elements and the more variation is a tool to discriminate the source composition. The variation diagram Th/Yb versus Ta/Yb (fig 4.19) shows relatively higher concentration of Th, compared to the OIT and MORB. This may indicate contamination with lower crust or metasomatism with sub continental lithosphere. Despite of the lower basalts, the other samples plot outside of the range between OIB and MORB. Comparing to the OIT or MORB which define a unity, the deviation of the sample from the source (~1) increases with increasing the evolution of the rock this may suggest there may be concurrent assimilation and fractional crystallization (AFC) during magma ascent with lower basalt, the least contaminated. However, based on the plot of 87Sr/86Sr to Fe2O3/MgO from the rocks of Amaro and Gamo reveal crustal contamination during fractional crystallization is improbable (George and Rogers 2002). Instead they used to classify Amaro basalts based on Δ8/4, and La/Nb and 87Sr/86Sr, and determined the one with La/Nb<1 as uncontaminated crust. Accordingly, the lower basalts of the Gidole horst have La/Nb>1, which suggests they are crustal contaminated.

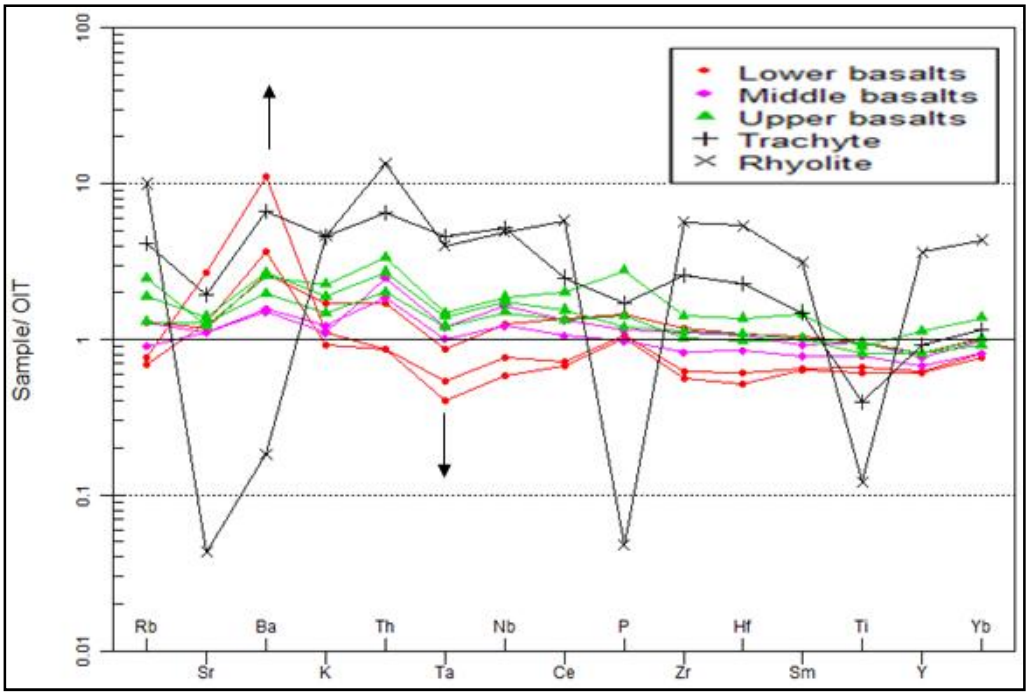

Figure 4.19. Spider diagram for the rocks of Gidole horst normalized to OIT (normalization from Wilson 2007)

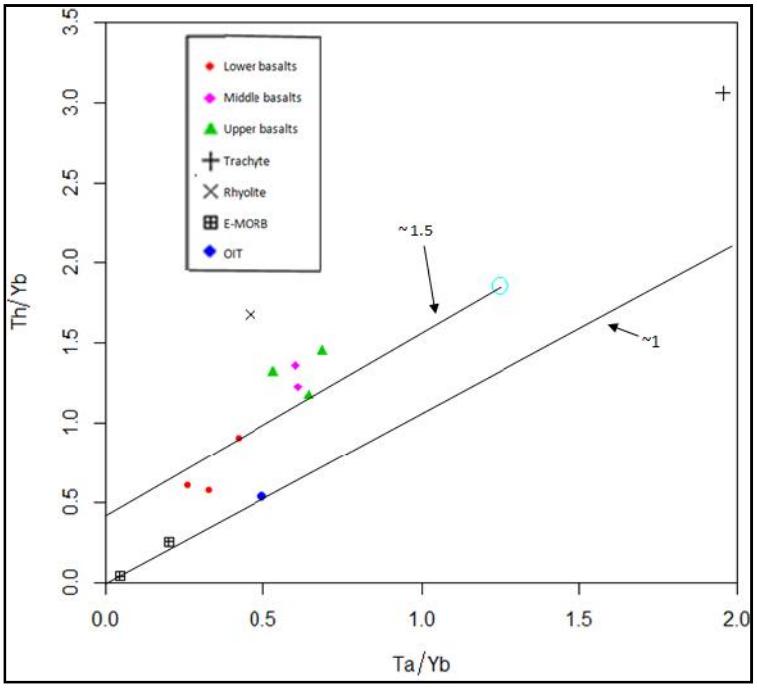

Figure 4.20. The variation diagram Th/Yb versus Ta/Yb for Gidole volcanic rocks. The large blue circle is OIB (OIT data from willison 2007, and OIB and MORB from sun and mcdonough 1989). These diagram used before by pearce (1983) to determine contamination.

5.1.2. Magma generation

The high concentration Ni and MgO in the lower basalt compared to the upper phase, is a base to select the lower basalt as primitive basalts (also George and Rogers 2002 considered lower Amaro basalt as primitive basalt) but not primary magma. The variation diagram of major oxide, the variation diagram of trace elements and the chondrite normalized REE diagram suggests the all the rocks have interlinked by crystal fractionation. Thus, the lower basalts are the oldest and most primitive from which the others are evolved by crystal fractionation. However, the fundamental problem is determining the source rock possible to form the primary magma (In these case no but primitive magma) the asthenosphere, the lithosphere mantle sources or the lower mantle.

The magmatic province in southwest Ethiopia characterized by episodic volcanism that become increasingly silica-under saturated through time. Rooney (2019) associate this shift in magma compositions from more silica-saturated to silica-under saturated with a decrease in the degree of extension. However, he argued that the initial melts in the rift exhibit silica-under saturation reflecting the initial destabilization and thinning of the lithospheric mantle while subsequent eruption after lithospheric thinning, the trend towards silica-saturated compositions reflects melting of the sub-lithospheric (i.e. convicting) mantle.

Therefore, the volcanic rocks of Gidole horst plotted with the MORB (fig 4.16) in the chondrite normalized REE diagram to test the existence of asthenosphere as source region in the generation of the rocks of Gidole horst basalts. So, basalts from Gidole horst are generally enriched with light-REE element similar with OIT, but not with E-MORB that have un-fractionated heavy REE element. Thus the fractionation of H-REE elements in both OIT and Gidole basalts despite of their fractionation indicates they were derived by relatively small degrees of partial melting of a source in which, garnet remains as a residual. Thus, the plot of the samples above 10 times the chondrite indicates they are in the transition between the spinel-garnet lherzolite (Dereje Ayalew et al., 2016). Rooney (2017) also reported the incompatible trace element depleted family of magmas (Type I) specifically, the Eocene Amaro basalt and the low titanium (LT) Oligocene flood basalt from NW Ethiopian plateau associated with a mantle plume source.

George and Roger (2002) tested similar rocks of the southern rift from Amaro horst north of the Chamo basin for their source rock using fractional melting model. Therefore the Miocene Amaro and Gamo basalts plot on the garnet source whereas Getra-Kele exclusively plot on the garnet free source. Similarly, the model of fractional melting of primitive mantle (fig 4.21) with a composition 55% olivine, 25% orthopyroxene, varying composition of clinopyroxene and garnet from 15 to 20% and from 0-5 respectively (an approximate to the average value garnet lherzolite given by Maaløe and Aoki 1977; Wilson 2007) show the same plot. However, all basaltic samples of Gidole horst plot on the garnet source between the two Amaro basalts of varying garnet source composition and, between the Gamo and Amaro basalts based on the degree of melting. That means, Gidole horst basalts have a nearly between 1 and 2% garnet specifically near to 1% garnet, whereas the Amaro basalts have a varying garnet composition. Thus, the plot of lower basalt with OIT indicates lower basalts have similar source rock with OIT basalt in the transitional Garnet lherzolite to the spinel lherzolite. This may suggest Gidole basalt rocks are plume originated rocks similar to OIB origin with small degree (<3%F) of transitional garnet source melting.

Accordingly, there is no rocks equivalent to the Getra-Kele and recently erupted basaltic rocks (Ebinger et al., 1993; George and Rogers 2002) in the Gidole basalts. The absence of equivalent rocks with Tosa Sucha volcanics in the Gidole horst is related with the shift of magnetism from border to the rift center (Ebinger el al., 1993; Rooney 2010; 20017). Similarly, George and Rogers (2002) related Getra-Kele basalts with the Tosa Sucha basalts, which will be a case for the absence of this rock in the Gidole horst. The Gamo basalts mimics with the middle basalts in the variation diagrams of Major oxides but have higher K2O compared to the middle basalts suggesting they are contaminated with the lower curst (Wilson 2007). The differences arise in the isotope signature between the Amaro basalts and Gamo basalts may be the result of crustal contamination. However, George and Roger (2002) determined the possible contamination is improbable. Therefore, the middle basalts are derived from lower basalts but not similar with Gamo basalts.

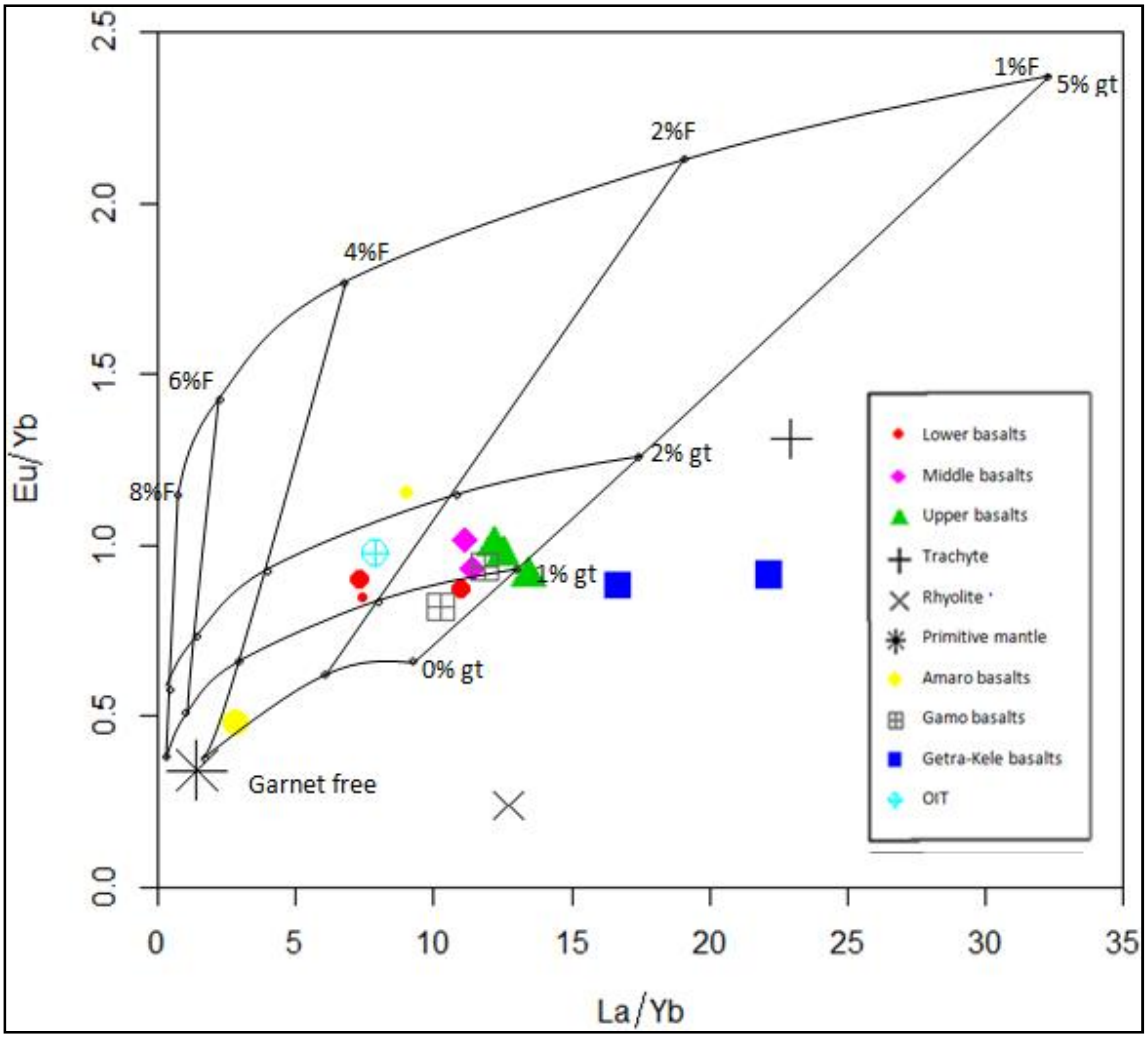

Figure 4.21. variation of Eu/Yb versus La/Yb of Gidole horst rocks compared with a fractional melting grid using primitive mantle as a source (data for primitive mantle is from Sun and Macdonough, 1989) and mantle composition of 55% olivine, 25% orthopyroxene and varying compositions of Clinopyroxene and Garnet from 15-20% and from 0-5% respectively. Data for Amaro, Gamo and Getra-Kele are from George and Rogers.

Co-variation of sodium andiron concentration was inferred to determine the depth and degree of melting in MORB (Klein and Langmuir 1987), and continental flood basalts (Turner and Hawkesworth 1995). Recently George and Roger used similar approach to determine the source and degree of melting in the least contaminated Amaro basalt. Consequently, Amaro basalts have a deep melting regime and small melt fraction than are required to generate MORB.

Fig 4.22 shows the variation of Y/Nb versus Zr/Nb to determine the source of the rocks with respect to the rocks whose source ware identified (data from Wilson 2007 and Sun and Mcdonough 1989). Assuming primitive mantle is a source for the MORB and OIB basalts, the most primitive sample of the Gidole horst plot near the OIT between OIT and MORB. These suggests the sample have shared the source of OIT with little modification with MORB source the asthenosphere or modification by lower crust as presented in fig 4.12 having low values of Ce/Pb and Nb/U combined with troughs observed on the spider diagram(fig 4.10). The lower basalts and OIT have high Zr/Nb ratio and low Y/Nb than the E-MORB indicating garnet play a role to differentiate among those elements where Y is retained back to the Garnet. This is because Garnet accommodates Y in its source region at low partial melting than Zr. The very low value of those ratios observed from the OIB, which plots with the more evolved magmas does not indicate OIB is fractionated, rather it indicate the high value of Nb.

The basalts from Gidole horst have High La/Nb and low Ti/Eu (not Shown) close to the chondritic ratios, suggesting that a titanite mineral does not play a role in the generation of those basalts (Weaver et al., 1988). Thus, higher La/Nb ratios of the samples reflect a mantle source characteristic. Many authors (Hart et al., 1989; Furman 2007; Dereje Ayalew 2006; Rooney et al., 2014; Dereje Ayalew et al., 2016) reported the existence of hydrous phase minerals in the source region in the Ethiopian rift system. Thus, the presence of hydrous phase minerals (phalgopite and amphibole) will result in the depletion of K and Rb relative to other elements. However, in the basaltic rocks of Gidole horst there is no depletion in those elements rather there is an enrichment of those elements especially in the lower basalts, indicating the absence of hydrous phase minerals in the source region. Instead of the presence of hydrous phase in the source region, the enrichments in the lower basalts indicate the existence of contamination with the crustal rocks.

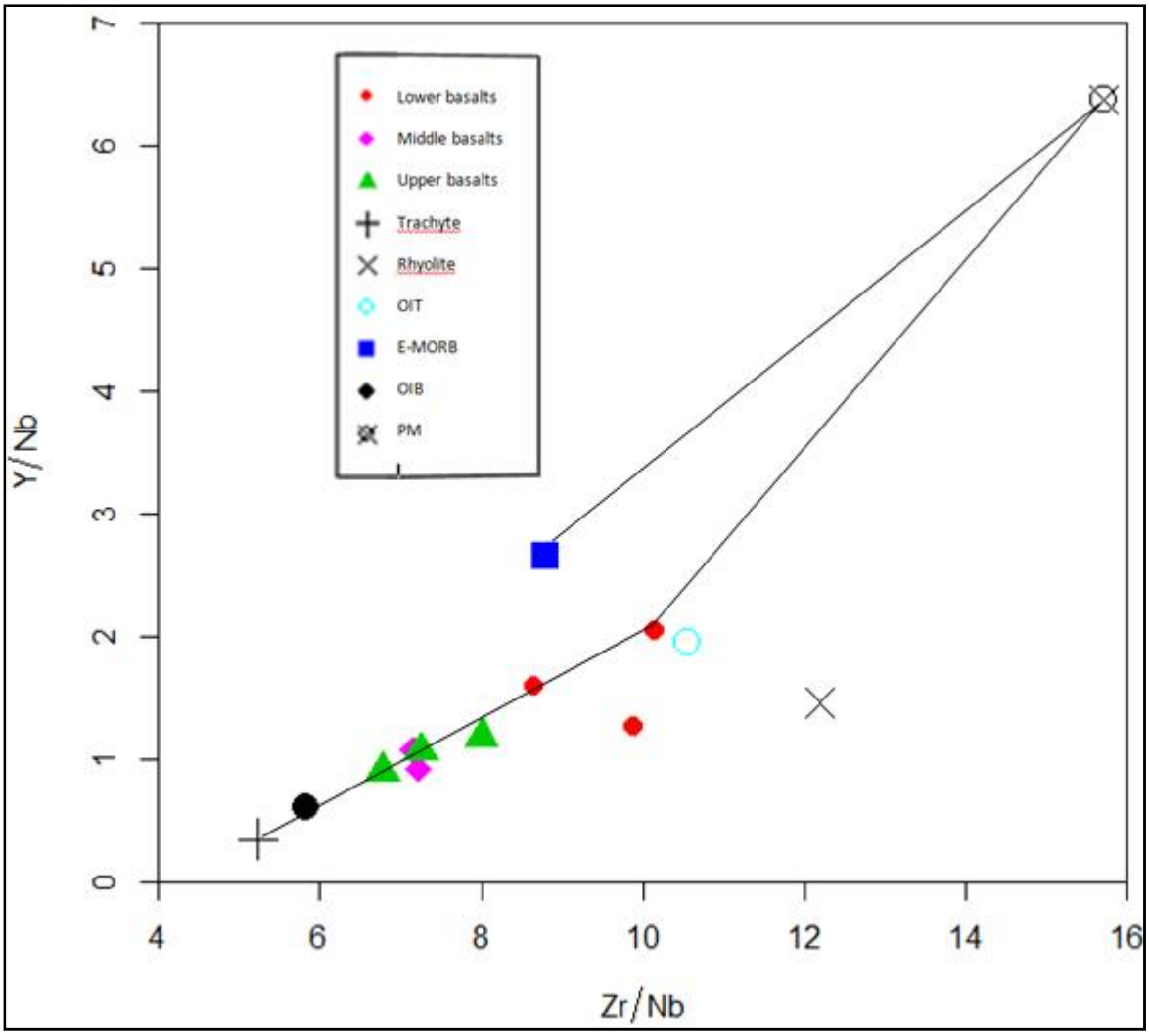

Figure 4.22. The variation diagram of Y/Nb versus Zr/Nb of Gidole hors rocks. The data for OIT from Wilson 2007, and for OIB, E-MORB and Primitive mantle (PM) from sun and Mcdonough(1989)

5.2. Petrogenesis of Gidole horst rhyolites

Different models have been proposed to explain and understand the genesis of the evolved rocks in the East African rift system. Some studies modeled the origin of peralkaline igneous activity associated with continental rifting stage as partial melting of local crust triggered by alkali-bearing volatiles (Macdonald et al. 1987; black et al 1997; Scaillet and MacDonald 2001). However, recent studies from Ethiopian rift system agree on the origin of peralkaline rocks by fractional crystallization of transitional basaltic parental melt with minor role for crystal contaminations (Dereje Ayalew et al., 2002; Peccerillo et al., 2003; 2007; Ronga et al., 2010). This is because local basement rocks are characterized by high LILE/HFSE and hence melting of

those rocks tend to preserve or increase the ratio, which is not now observed in the rocks (Peccerillo et al., 2003; 2007). While fractional crystallization model explain, some geological characteristics of the per-alkaline rocks but fail to explain the lack of rocks with intermediate composition (Peccerillo et al., 2003). Such bimodal composition of lava has in the past been used to argue against crystal fractionation models (e.g. Cox.et al., 1979). Nevertheless, for some of these bimodal suites there is strong geochemical evidence (trace and radiogenic isotopes) to indicate that crustal rocks are involved in the petrogenesis of the more silica-rich members (Peccerillo et al., 2003; 2007).

Volcanic rocks of Gidole horst also show the absence of intermediate rocks so-called daily gap. The strong curved trends for several major and trace element diagrams support fractional crystallization start from lower basalt to the most evolved silicic rock. More over the nearly constant ratio La/Hf and Zr/Ce (fig 4.23) reported before by Barbari et al. (1975) as fractionation -controlled the evolution also support the fractionation of those silicic rocks. However, some deviations observed on the major and trace element diagram especially between trachyte and rhyolite suggest the existence of contamination or extensive crystal fractionation of some minerals. For example, the very low concentration of Na in the most evolved rhyolite with high loss of index may suggest secondary alteration of these rocks with water (Gezahegn Yirgu et al., 1999; Peccerillo et al., 2003). This low concentration is may be also due to the intensive sodic plagioclase fractionation (Peccerillo et al., 2003) by trachyte as it has a very high concentration of Na2O together with Al2O3 and Ba among the samples that resulted strong depletion of those elements in the more evolved rocks. The latter is more convincing; because the secondary alteration tends to increase, Al2O3 rather than decreasing the concentration as Al2O3 is in sensitive to alteration (consider Bauxite).If this is the case, the higher depletion of sodium in the rhyolite will occur if and only if the fractionating minerals have the higher concentration of Sodic plagioclase and, the liquid remaining should be low.

Therefore, from the crystal fractionation model for compatible and incompatible minerals (fig 4.24), the liquid remaining from trachyte is < 2% and from thin section study and CPIW norm (not shown) the trachyte has higher concentration of minerals plagioclase (albite). Similarly, some variations in trace elements and REE element diagrams of these two evolved product may arise from these point of view. The negative Sr concentration observed in the trachyte does not

contradict the fractionation Na-plagioclase by itself as Sr substitute Ca in plagioclase rather than sodium and this depletion also seen in the middle, upper basalts indicating more Sr is consumed in the previous rocks. In addition, the higher concentration of barium in the trachyte is due to the possible substitution of Na by Ba (winter 2014).

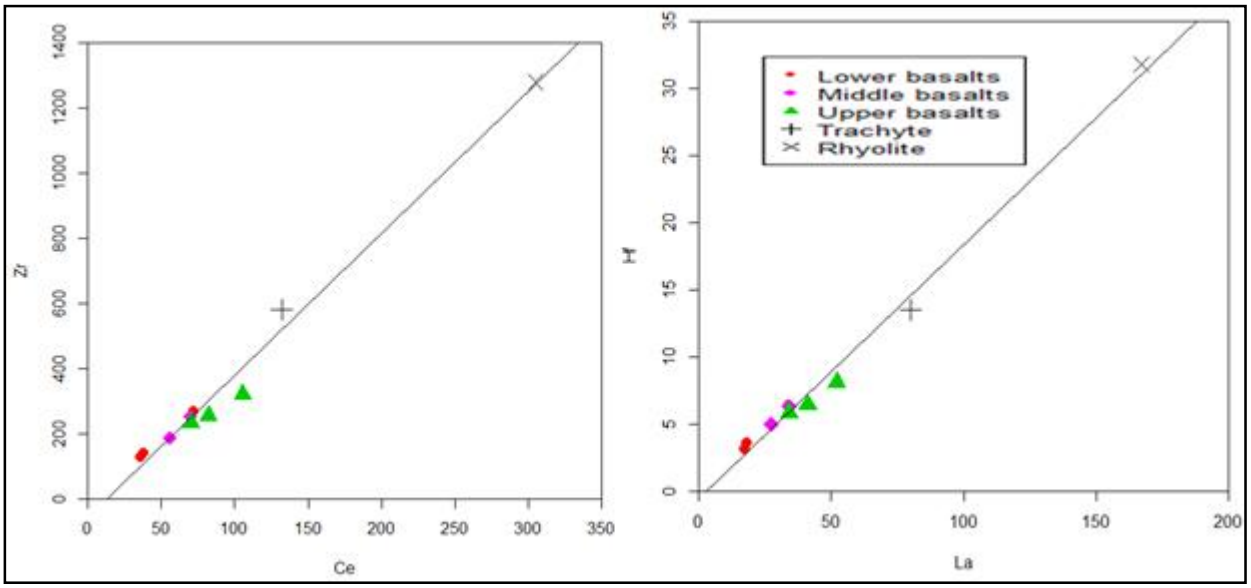

Figure 4.23. Variation diagram of Zr versus Ce and Hf versus La (PPm) for basaltic rocks of Gidole horst

On the primitive mantle normalized diagram the rhyolitic rocks of the Gidole have strong trough at Ba, Sr,Ti and p where similar andesitic and rhyolitic rocks from Yemen (Baker et al 1996b) and Ethiopia (Dereje et al 2002) show negative concentration of those elements. The negative concentration of Ba &Sr together with Eu anomaly observed in the chondrite-normalized REE diagram in the rhyolite strongly suggests the extensive fractionation of feldspar at this stage (Depaola 1981; Baker et al., 1996b; Wilson2007).

Model created for fractional crystallization of compatible and incompatible elements assuming the most primitive sample analyzed as starting magma (fig 4.18). From this model, the compatible element (in this case Sr) decreases with increased crystal fractionation and the incompatible elements (Rb and Zr) increases with increased fractionation. Accordingly, those incompatible elements enriched in the more evolved rocks and compatible elements depleted. Furthermore, the constant ratio and sub parallel patterns without inter-element fractionation suggest the rocks are controlled by crystal fractionation.

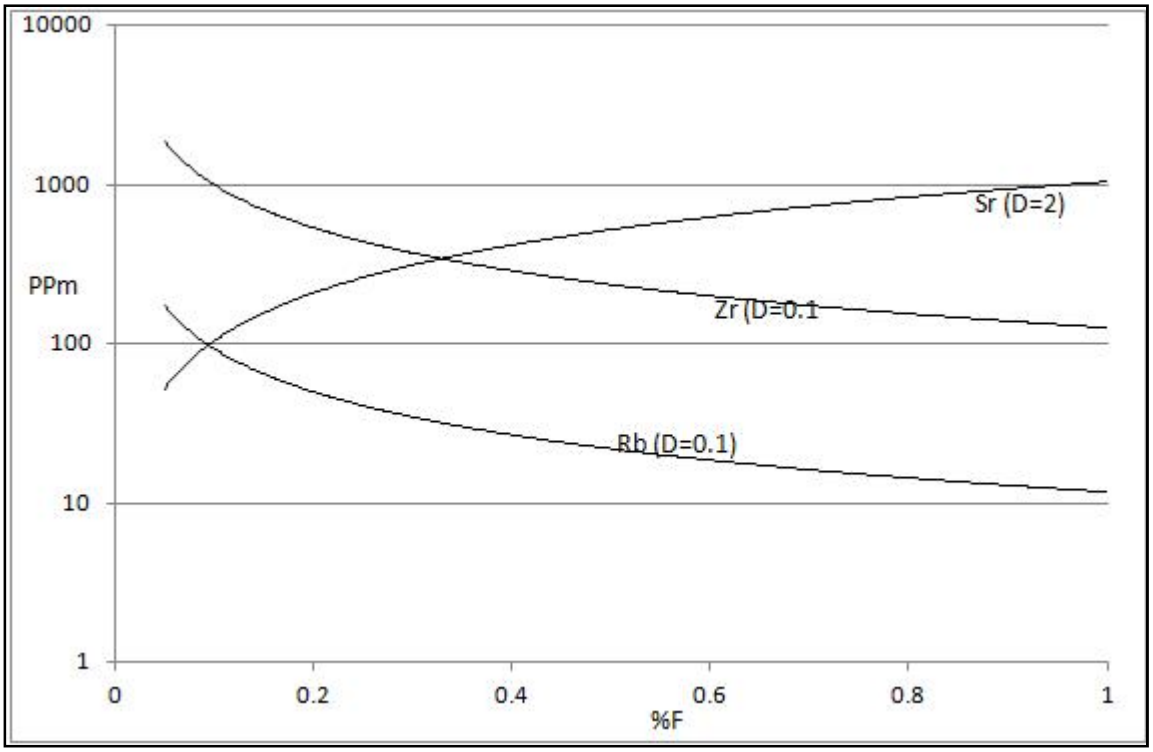

Figure 4.24. Fractional crystallization models for the Gidole horst rocks assuming the most primitive sample as starting. Vertical line gives absolute abundance of the concentration of residual liquid. %F indicates weight fraction of residual

However the stratigraphic position of the felsic rocks does not support crystal fractionation. Instead their plot outside of the garnet source allow to constrain they are derived from the underlying rocks. So, melting of the local basement rocks are characterized by high LILE/HFSE (Peccerillo et al., 2003; 2007) and hence is not now observed in the rocks. Therefore a detail study of the felsic rock is recommended.

Chapter six

6. Conclusion and recommendations

6.1. Conclusion

The volcanic rocks of Gidole horst have a considerable range of differentiation among the three phases of eruptions. The lower basalt is coarse grained with phenocrysts of olivine, plagioclase and microphenocrysts of olivine, plagioclase, pyroxene and opaque. The middle and the upper basalts have less olivine and consist of plagioclase, pyroxene and opaque and amphibole appear in the upper basalts. The felsic rock specifically trachyte have a plagioclase, less pyroxene and opaque minerals. Where the felsic tuffs have less a plagioclase, rather it has a larger crystal of sanidine together with quartz and rock fragments.

The basaltic rocks of Gidole horst have a limited range of SiO_2 and an appreciable range of MgO. According to the TAS classification, all rocks plot in the area of transition basalt on the side of alkaline field except the rhyolitic ignimbrite. The exclusive plot of rhyolite in the tholeiitic field is due to the extensive fractionation of sodic plagioclase by trachyte that is a reason for the low concentration of sodium in rhyolite. From variation diagram of major oxide versus MgO, the order of fractionating mineral is olivine, plagioclase and apatite in the lower basalt and, olivine, pyroxene and Fe-Ti oxide in the latter phases. The variation diagram of Ni versus MgO shows a rapped drop of Ni concentration from lower to the middle basalts supports the fractionation of olivine.

The stratigraphic position, petrographic and geochemistry support the presence of crystal fractionation among the volcanic rocks of Gidole horst. The decrease in MgO and increase of Sio2 on the major oxide, the increase of incompatible elements with decrease of MgO on the variation diagram and the sub-parallel pattern with limited intermixing on the chondrite normalized REE shows the existence of crystal fractionation. The strong relationship of the rocks with Amaro-Gamo basalts and the absence of equivalent rock with the Getra-Kele basalts from the Gidole horst help to draw a conclusion that the rocks are co-genetic formed by fractional crystallization of the source. The variation diagram of incompatible element versus incompatible elements produces a straight line and support the existence of crystal fractionation. Moreover the nearly constant ratios produce by the basalts is an evidence for crystal fractionation.

However, the basalts show a trough between Ba and La of the basaltic rocks with K peak in the lower basalts indicate the rocks are crustal contaminated. Therefore, the basalts show a low Ce/ Pb ratio except one sample from the lower basalts and from the upper basalts. The basalts of Gidole horst normalized to the OIT basalts show the enrichment of Ba and depletion of Ta supports the involvement of sub-continental lithosphere for the rocks come from mantle. Even though the volcanic rocks of Gidole horst have higher Ba/Nb and Low Ce/Pb, they have a ratio of La/Pb similar to OIT that is higher than the MORB and OIB indicating similar source with OIT and later modification by lower curst.

The basaltic rocks of Gidole horst show a strong correlation starting from lower basalt to the upper basalts. They have OIB (specifically OIT) like signatures, suggesting they are co-genetic and evolved from homogenous mantle source. Furthermore, the basalts show sub parallel pattern with uniform LREE enriched and HREE depleted in the mantle normalized diagram, indicating they were derived by relatively small degrees of partial melting of a source in which, garnet remains as a residual on the transitional to spinel. Based on the sodium and iron concentration, the lower basalts have a deep melting regime and small melt fraction than are required to generate MORB. The high concentration of Sr and Ba in the lower basalts suggests shallow level of crystal fractionation in which the plagioclase is stable.

The petrographic and geochemical signatures of the Gidole horst rhyolitic rocks suggest they were derived from the basalts by fractional crystallization. As a result, the very low concentrations of Sr, Ti, and P opposite to the basaltic rocks suggest the fractionation of apatite, plagioclase and Fe-Ti oxides. Furthermore, the rocks have higher concentration of the incompatible elements and lower compatible elements indicating the presence of crystal fractionation. However, their stratigraphic position is between the basalts and the trachyte on above the felsic tuff does not rely on the crystal fractionation. Instead the plot of those rocks with outside of the Garnet source will allow those rocks formed by melting of the underlying rocks.

6.2 Recommendations

Based on the petrographic study, major and trace element variation the volcanic rocks show the signature of Crystal fractionation and to understand the evolution of the volcanic rocks of Gidole horst fractional crystallization model has been introduced in this study. However, to test such

evolution and their source rock, detailed trace and radiogenic isotopic studies of extensive stratigraphic section would be required. In addition to these mineral compositions of each minerals has to be analyzed for better understanding of the evolution of the rocks. The age of each rock unit (i.e. each eruption of the basalts and the felsic rocks) has to be determined.

The petrogenesis of the more evolved magma from transitional nature of Ethiopian basalts remains unsolved. In some instances major, trace and isotope data support their evolution by fractional crystallization of the basaltic magma (Barberi et al., 1975; Peccerillo et al., 2003, Dereje et al., 2002). However, the lack intermediate magma during fractional crystallization and an emplacement of huge Silicic magma argue against the simple fractional model. Instead it introduce to the partial melting of Crystal rocks. To understand the evolution of silicic magma of Gidole horst (as well as Southern main Ethiopian rift) detail study of under laying metamorphic rocks, trace element, and radiogenic isotope is needed. Furthermore, the effect of assimilation during magma assent has to be covered using isotope data.

Bibliography

Abbate, E., & Sagri, M. (1980). Volcanites of the Ethiopian and Somalian plateaus and major tectonic lines. Atti dei Convegni Lincei, 47, 219-227.

Arndt, N., Chauvel, C., Czamanske, G., & Fedorenko, V. (1998). Two mantle sources, two plumbing systems: tholeiitic and alkaline magmatism of the Maymecha River basin, Siberian flood volcanic province. Contributions to Mineralogy and Petrology 133, 297-313.

Baker, J., Snee, L., & Menezies, M. (1996a). A brief Oligocene period of flood volcanism in Yemen; implications for the duration and rate of continental flood volcanism at the Afro-Arabian triple junction. Earth planet. Sci. Lett 138, 39-55.

Barberi, F., Ferrara, G., Sentacroce, R., Treuil, M., & Varet, J. (1975). A transitional basalt-pantellerite sequence of fractional crystallization, the Boina Centre (Afar Rift, Ethiopia). J Petrol 16, 22-56.

Black, S., Macdonald, R., & Kelly, M. (1997). Crustal origin for peralka-line rhyolites from Kenya: evidence from U-series disequilibria and Th isotopes. J Petrol 38, 277-297.

Bosworth, W., & Morley, C. (1994). Structural and stratigraphic evolution of the Anza rift, Kenya. Tectonophysics 236, 93-115.

Civetta, L., D'Antonio, M., Orsi, G., & Tilton, G. (1998). The geochemistry of volcanic rocks from Pantelleria island, Sicily Channel: petrogenesis and characteristics of the mantle source region. petrol 39, 1453-1491.

Cox, K. (1985). Geochemical stratigraphy of the Deccan Traps, at Mahabaleshwar, Western Ghats, India, with implication for open system magimatic processes. J.petrol, 26, 355-77.

Davidson, A. (1983). Reconnaissence Geology and Geochemistry of part of Illubabor, Kefa, Gamogofa and Sidamo. Ministry of mines and energy, Ethiopian Institute of Geological Survey 2, 1-89.

Depaolo, D. (1981). Trace element and isotopic effect of combined wallrock assimilation and fractional crystallization. Earth Planet. Sci. Lett. 53, 189-202.

Dereje, Ayalew, & Gibson, A. (2009). Head-to-tail transition of the Afar mantle plume: Geochemical evidence from a Miocene bimodal basalt–rhyolite succession in the Ethiopian Large Igneous Province. Lithos 112, 461-476.

Dereje, Aayalew, Jung, s., Romer, R., Kersten, F., Pfander, J., & Gorbe-Schonberg, D. (2016). Petrogenesis and origin of modern Ethiopian rift basalts: constraints from isotope & trace element geochemistry. lithos, 258-259, 1-14.

Dereje, Ayalew, P., B., Marty, B., Reisberg, L., Gezahegn, Yirgu, & Pik, R. (2002). Source, genesis, and timing of giant ignimbrite deposits associated with Ethiopian continental flood basalts. Geochimica et Cosmochimica Acta 66, 1429-1448.

Ebinger, C., Yemane, T., Giday, Woldegabriel, Aronson, J., & Walter, R. (1993). Late Eocene-recent volcanism in the southern main Ethiopian rift. J.Geol. Soc. 150, 99-108.

Ebinger, C., Yemane, T., Harding, D., Kelley, S., & Rex, D. (2000). Rift deflection, migration and propagation: Linkage of the Ethiopian and Eastern rifts, Africa. GSA Bulletine 112(2), 163-176.

Furman, T. (2007). Geochemistry of East African Rift basalts. Journal of African Earth Sciences 48, 147-160.

George, R., & Rogers, N. (2002). Plume dynamics beneath the African plate inffered from the geochemistry of the tertiary basalts of southern Ethiopia. Contrib mineral petrol, 144, 286-304.

Gezahegn, Yirgu, Dereje, Ayalew, Peccerillo, A., Donati, M., & Donato, P. (1999). Fluorine and chlorine distribution in the volcanic rocks from the Gedemsa volcano, Ethiopian Rift Valley. Acta Volcanologica, 11, 169-176.

Giday, Woldegabriel, & Aronson, J. (1987). Chow Bahir Rift — A Failed Rift in Southern Ethiopia. Geology 15, 430-433.

Giday, Woldegabriel, Yemane, T., White, T., Asfaw, B., & Suwa, G. (1991). Age of volcanism and fossils in the Burji-SOyoma area, Amaro horst, southern main Ethiopian rift. J. Afr. Earth Sci 13, 437-447.

Hart, W., Giday, Woldegabriel, Walter, R., & Mertzman, S. (1989). Basaltic volcanism in Ethiopia — constraints on continental rifting and mantle interactions. Journal of Geophysical Research-Solid Earth and Planets 94, 7731-7748.

Hofmann, A. (2003). Sampling mantle heterogeneity through oceanic basalts: isotopes and trace elements. In: Carlson, R.W. (Ed), Treatise on Geochemistry. The Mantle and Core 13, 61-101.

Hofmann, A., Jochum, K., Seufert, M., & White, W. (1986). Nb and Pb in oceanic basalts - new consraints on mantile evolution. Earth and Planetery Science Letters 79, 33-45.

Irvine, T., & Baragar, W. (1971). A guide to the chemical classification of the common volcanic rocks. canadian Journal of Earth science 8(1971), 523-548.

Jones, P. (1976). Age of the lower flood basalts of the Ethiopian plateau. Nature 261, 567-569.

Kieffer, B., Arndt, N., Lapierre, H., Bastien, F., Bosch, D., Pecher, A., . . . Mougniot, C. (2004). Flood and shield basalts from Ethiopia: magmas from the African superswell. Journal of petrology 45, 793-834.

Klein, E., & Langmuir, C. (1987). Global correlations of ocean ridge basalt chemistry with axial depth and crustal thickness. J Geophys Res 92, 8089-8115.

Le Bas, M., Le Maitre, R., Streckeisen, A., & Zanettin, B. (1986). A chemical classification of volcanic rocks based on total alkali–silica diagram. Journal of petrology 27, 745-750.

Levitte, D., Columba, J., & Mohr, P. (1974). Reconnaissance geology of the Amaro horst, southern Ethiopian rift. Geol.Soc.Am.Bull 85, 417-422.

Maaloe, S., & Aoki. (1977). The Major element composition of the upper mantile estimated from the composition of lherzolites. Contrib.Mineral.Petrol. 63, 161-73.

Macdonald, R. (1974). Nomenclature and petrochemistry of the peralka-line oversaturated extrusive rocks. Bull Volcanol 38, 498-516.

Macdonald, R., Davies, G., Bliss, C., Leat, P., Bailey, D., & Smith, R. (1987). Geochemistry of high-silica rhyolites, Naivasha, KenyaRift Valley. J Petrol 28, 979-1088.

Nelso, D., McCulloch, M., & Sun, S. (1986). The origins of ultrapotassic rocks as inferred from Sr, Nd and Pb isotopes. Geochem. Cosomochim. Acta 50, 231-45.

Pearce, J. (1983). Role of Sub-continental lithosphere in magima genesis at active continenetal margins. (C. Hawkesworth, & M. Norry, Eds.) Nantwich, Cheshiro: Shiva publications.

Peccerillo, A., Barberio, M., Gezahegn, Yirgu, Dereje, Ayalew, Barbieri, M., & Wu, T. (2003). Relationship between mafic and peralkaline silicicmagmatism in continental rift settings: a petrological, geochem-ical and isotopic study of the Gedemsa volcano, Central Ethiopian Rift. J Petrol 11, 2003-2032.

Peccerillo, A., Donati, C., Salto, A., Orlando, A., Gezahegn, Yirgu, & Dereje, Ayalew (2007). Petrogenesis of silicic peralkaline rocks in the Ethiopian rift: geochemical evidence and volcanological implications. J Afr Earth Sci 48, 161-173.

Philippon, M., Corti, G., Sani, F., Bonini, M., Maria-Laura, Belestrieri, . . . Cloetingh, S. (2014). Evolution, distribution and characteristics of rifting in southern Ethiopia. Tectonics 33, 485-508.

Pik, R., Marty, B., Carignan, J., Gezahegn, Yirgu, & Teklewold, A. (2008). Timing of East African Rift development in southern Ethiopia: implication for mantle plume activity and evolution of topography. Geology 36, 167-170.

Rogers, N. (2006). Basaltic magmatism and the geodynamics of the East African Rift System. Geological Society London Special Publications 259, 77-93.

Ronga, F., Lustrino, M., Marzoli, A., & Melluso, L. (2010). Petrogenesis of a basalt-comendite-pantellerite rock suite: The Boseti Volcanic Complex (Main Ethiopian Rift). Miner. Petrol 98, 227-243.

Rooney, T. (2010). Geochemical evidence of lithospheric thinning in the southern Main Ethiopian Rift. Lithos 117, 33-48.

Rooney, T. (2017a). The Cenozoic magmatism of East-Africa: Part I — Flood basalts and pulsed magmatism. Lithos 286, 264-301.

Rooney, T. (2019). The Cenozoic Magmatism of East Africa: Part V– Magma sources and Processes in the East African Rift. Lithos.

Rooney, T., Furman, T., Bastow, I., Dereje, A., & Gezahegn, Y. (2007). Lithospheric modification during crustal extension in the Main Ethiopian Rift. J Geophys Res 112, 3889-3910.

Scaillet, B., & Macdonald, R. (2001). Phase relations of peralkaline silicic magmas and petrogenetic implications. J petrol 42, 825-845.

Sun, S., & McDonough, W. (1989). Chemical and isotopic systematics of oceanic basalts: implications for mantle composition and processes. In: Saunders, A.D. (Ed.), Magmatism in the Ocean Basins. . Geological Society, 313-345.

Trua, T., Daniel, C., & Mezzuoli, R. (1999). Crustal control in the genesis of Plio-Quaternary bimodal magmatism of the Main Ethiopian Rift (MER): geochemical and isotopic (Sr, Nd, Pb) evidence. Chemical Geology, 155, 201-231.

Turner, S., & Hawkesworth, C. (1995). The nature of the sub-continental mantle: constraints from the major-element composition of continental flood basalts. Chem Geol, 120, 295-314.

Vojetech, J., Colin M., F., & Vojtech, E. (2006). Interpretation of whole-rock geochemical data in igneous geochemistry: introducing Geochemical Data Toolkit (GCDkit). Journal of petrology, 47, 1255-1259.

Wilison, M. (2007). Igneous petrology: A Global Tectonic Approach (Vol. 480). Netherland: springer.

Winter, D. (2014). Principles of Igneous and Metamorphic Petrology (second edition ed.). England: Preason.

WV, B. (1984). Cosmochemistry of the rare earth elements: meteorite studies. In: Henderson P (ed) Rare earth element geochemistry. Elsevier, 63-114.

Yemane, T., & Yohunie, T. (1987). Geological report on sub-sheets A, B. and C (Agere Mariam, NG-37-10). Ethiopian Institute of Geological Surveys, Addis Ababa.

Appendix

1. Petrographic description for the Gidole horst volcanic rocks

Rock name	sample code	Location	Elevation	Description
basalt	p1	326677, 624344	1239	It is porphyritic basalt in which the phenocrysts are olivine and plagioclase coexists. The plagioclase is euhedral to sub-hederal and there is change in composition from core to the rim. The olivine is altered to iddingsite along its rims. The microphenocrysts are olivine, plagioclase and pyroxene and opaque proportionally plagioclase 40%, olivine 35% pyroxene 10% and opaque 15%.
basalt	P3	326549, 624416	1304	Olivine phyric basalt with microphenocrysts of olivine, plagioclase, pyroxene and opaque. The olivine phenocrysts are euhedral to subhedral and some shows an alteration along their rims. The proportions of the minerals are olivine 45%, plagioclase 35%, pyroxene 8% and opaque 12%.
basalt	pL	326297, 625664	1369	It contains micro-vein in the thin section and this vein is felsic in composition, composed of quartz and plagioclase. The host rock is consists of microphenocrysts of plagioclase, pyroxene, olivine and opaque.
Ignimbrite	Gs1	325452, 624248	1388	The ignimbrite contains euhedral to subhedral phenocrysts of volcanic glass, sanidine, and quartz embedded in fine-grained groundmass of feldspar and biotite. The phenocrysts and ground mass are oriented to the same direction indicating the stress direction during the formation these rocks. Sanidine sometimes shows a simple contact twin and has a poikilitic texture enclosing the rock fragments.
tuff	Gs2	325339, 624298	1394	The felsic tuff samples contain volcanic fragments, feldspar and free quartz. The proportion of rock fragment is >50%.
basalt	Gs5	325298, 624145	1413	It is very fine grained with sub-trachy texture. It contains plagioclase (40%), pyroxene (35%) and olivine (5%) and opaque (20%).
basalt	GS11	325094, 624344	1505	It is very fine grained with sub-trachy texture in which the plagioclase orients in the same direction. It contains plagioclase (37%), pyroxene (35%) and olivine (3%) and opaque (25%). The opaque proportions in those basalts are high and relatively larger compared with the others.

trachyte	Ts	326517, 626045	1548	Trachyte is very fine grained with trachytic texture defined by <1mm long, aligned plagioclase lath. It contains plagioclase, amphibole and opaque minerals. The proportion of plagioclase is higher than the remaining minerals.
basalt	s 10	322643, 623941	1642	It is very fine grained with sub-trachy texture
basalt	s 9	321935, 623760	1784	It contains microphenocrysts of plagioclase, pyroxene and opaque with the groundmass of the same minerals. Olivine is subhedral to euhedral. The crystallization sequence is olivine,- clinopyroxene – plagioclase.
basalt	s 7	321266, 623551	1905	It is very fine grained with the minerals of plagioclase, pyroxene, opaque and few olivines.
basalt	sample 1	317179, 624835	2355	It is the upper most basalt contains microphenocrysts of plagioclase, pyroxene and opaque with a ground mass of the same minerals and olivine.
basalt	GAS 1	322829, 619268	1566	The lower most basalt contains more olivine with plagioclase with occasional 2-3mm clinopyroxene forming ophitic texture where the oikocryst pyroxene encloses a lath shaped plagioclase. The plagioclase in these flows is lath shaped and show a preferential orientation, which may have resulted from flow of magma before solidification. Olivine is altered to iddingsite along its rims.
basalt	GAS 3	322659, 620530	1637	It contain olivine and plagioclase phenocrysts and, with micro phenocrysts of plagioclase, olivine and pyroxene. The ground mass is composed of the same minerals together with opaque mineral. Olivine is altered to iddingsite along its rims. Some plagioclase show normal compositional zoning and oscillatory zoning occurs in the plagioclase phenocrysts
basalt	GAS 6	322450, 621919	1714	It has micro-vein composed of quartz and plagioclase parallel to the sub-trachy texture of plagioclase. It consists of plagioclase, pyroxene, olivine and pyroxene.

2. Major oxide Data recalculated on volatile freebase

	Lower basalts			Middle basalts		Upper basalts			Trachyte	Rhyolite
Oxides %	P1	GAS-3	PL	GS- 5	GS-11	Gar-1	S 9	S 7	TS	GS-1
SiO_2	47.51	46.76	47.32	47.08	48.47	48.05	50.1	49.96	62.49	76
TiO_2	2.19	2.38	3.45	3.5	2.85	3.42	2.93	3.23	1.44	0.44
Al_2O_3	15.84	15.9	15.18	14.08	14.3	13.64	14.1	13.87	17.93	11.06
Fe_2O_3	13.69	13.83	15.18	16.37	14.56	15.7	14.26	14.78	3.92	5.56
MnO	0.18	0.2	0.19	0.21	0.2	0.24	0.2	0.23	0.06	0.1
MgO	7.15	7.62	4.81	4.73	5.37	4.66	4.35	3.59	0.45	0.19
CaO	8.69	8.95	8.21	9.14	9.38	8.99	8.39	7.85	3.89	0.45
Na_2O	3.09	3.06	3.62	3.48	3.45	3.49	3.62	3.49	5.41	2.63
K_2O	0.86	0.71	1.32	0.85	0.94	1.13	1.45	1.73	3.49	3.55
P_2O_5	0.43	0.45	0.61	0.48	0.41	0.59	0.5	1.16	0.71	0.02
Cr_2O_3	0.022	0.019	0.005	0.002	0.009	0.004	0.006	0.002	0.002	0.003
SrO	0.11	0.05	0.05	0.05	0.04	0.05	0.05	0.05	0.08	<0.01
BaO	0.24	0.08	0.06	0.03	0.03	0.04	0.05	0.06	0.14	<0.01
Total	100	100	100	100	100	100	100	100	100	100
LOI	3.9	2.52	2.8	0.85	1.61	0.3	0.28	1.66	1.14	7.2

3. CIPW (wt %) norm for the rocks of Gidole horst

Minerals	**P1**	**PL**	**GS- 1**	**GS- 5**	**GS-11**	**S 9**	**S 7**	**GAS-3**	**TS**	**GAr-1**
Quartz	1.095	1.515	45.933	3.041	2.849	4.855	7.231	0.000	10.740	3.749
Corundum	0.000	0.000	2.120	0.000	0.000	0.000	0.000	0.000	0.000	0.000
Orthoclase	5.082	7.801	20.979	5.023	5.555	8.569	10.224	4.196	20.625	6.678
Albite	26.147	30.631	22.254	29.447	29.193	30.631	29.531	25.893	45.778	29.531
Anorthite	26.811	21.272	2.102	20.287	20.756	17.941	17.070	27.552	14.331	18.215
Diopside	5.114	3.270	0.000	8.215	10.864	8.558	3.072	4.985	0.000	8.998
Hypersthene	15.441	10.466	0.473	7.975	8.341	6.869	7.519	16.614	1.121	7.437
Olivine	1.002	0.601	0.000	0.000	0.000	0.000	0.000	1.040	0.000	0.000
Ilmenite	0.385	0.406	0.214	0.449	0.428	0.428	0.492	0.428	0.128	0.513
Titanite	4.879	7.944	0.000	8.012	6.444	6.640	7.294	5.290	0.232	7.732
Rutile	0.000	0.000	0.328	0.000	0.000	0.000	0.000	0.000	1.279	0.000
Apatite	1.019	1.445	0.047	1.137	0.971	1.184	2.748	1.066	1.682	1.397
Sum	86.972	83.552	94.451	83.585	85.402	85.676	85.181	86.064	95.915	84.251